JOURNAL OF GEOPHYSICAL RESEARCH, VOL. 107, NO. D23, 8177, doi:10.1029/2001JD000577, 2002

Middle atmosphere Kelvin waves observed in Cryogenic Infrared Spectrometers and Telescopes for the Atmosphere (CRISTA) 1 and 2 temperature and trace species

A. K. Smith

Atmospheric Chemistry Division, National Center for Atmospheric Research, Boulder, Colorado, USA

P. Preusse[1] and J. Oberheide[2]

Department of Physics, University of Wuppertal, Wuppertal, Germany

Received 2 March 2001; revised 5 September 2001; accepted 10 September 2001; published 18 September 2002.

[1] A number of tropical perturbations that have all the characteristics of Kelvin waves are identified in temperature measurements from the two flights of the Cryogenic Infrared Spectrometers and Telescopes for the Atmosphere (CRISTA) instrument. The background wind conditions during the two flights were quite different due to the different phases of the quasi-biennial oscillation (QBO), and there were differences in the Kelvin waves observed. During each flight, there were several different zonal wave numbers and/or frequencies present simultaneously. The observed waves conform well to theory. In particular, lower-frequency waves are confined to the lower stratosphere, while higher-frequency waves appear in the upper stratosphere and mesosphere; the waves are centered on the equator; and the frequency and structure satisfy the dispersion relation. Wave signals also appear in several stratospheric trace species: O_3, CFC-11 ($CFCl_3$), HNO_3, N_2O, and CH_4. The sense of the correlation of these trace species perturbations with temperature (negative for CFC-11, N_2O, and CH_4; positive for lower stratospheric HNO_3 and O_3) confirms that vertical velocity is responsible for the perturbations. There is a shift in the relative phases as photochemical processes become more important with increasing altitude. Upper stratospheric ozone correlates negatively with temperature due to temperature-dependent reaction rates that destroy ozone. *INDEX TERMS:* 0341 Atmospheric Composition and Structure: Middle atmosphere—constituent transport and chemistry (3334); 3334 Meteorology and Atmospheric Dynamics: Middle atmosphere dynamics (0341, 0342); 3374 Meteorology and Atmospheric Dynamics: Tropical meteorology

Citation: Smith, A. K., P. Preusse, and J. Oberheide, Middle atmosphere Kelvin waves observed in Cryogenic Infrared Spectrometers and Telescopes for the Atmosphere (CRISTA) 1 and 2 temperature and trace species, *J. Geophys. Res.*, *107*(D23), 8177, doi:10.1029/2001JD000577, 2002.

1. Introduction

[2] Kelvin waves are an important class of atmospheric perturbation because of their frequent appearance in the tropical middle atmosphere and their role in the momentum balance there. They have been shown to make significant contributions to driving the mean wind oscillations that dominate the tropical middle atmosphere climatology: the quasi-biennial oscillation (QBO) in the lower stratosphere and the semiannual oscillations (SAO) near the stratopause and mesopause. Kelvin waves have distinct features that make them straightforward to identify in global observations. There have been a number of observations of Kelvin waves from limb-viewing satellite temperatures [*Salby et al.*, 1984; *Hitchman and Leovy*, 1988; *Canziani et al.*, 1994; *Shiotani et al.*, 1997] and they have also been detected in satellite wind measurements [*Srikanth and Ortland*, 1998; *Lieberman and Riggin*, 1997]. In addition, Kelvin waves have been found in tropical radiosonde [*Wallace and Kousky*, 1968; *Holton et al.*, 2001], rocket [*Hirota*, 1979] and radar [*Riggin et al.*, 1997] data.

[3] *Holton and Lindzen* [1968] demonstrated that momentum deposited by Kelvin waves would force easterly acceleration of the zonal winds. There have subsequently been numerous studies investigating the role these waves play in models and in the atmosphere. They are believed to play significant roles in the driving of the QBO [*Takahashi and Boville*, 1992; *Canziani and Holton*, 1998] and the SAO [*Hirota*, 1979; *Dunkerton*, 1979, 1982; *Hitchman and Leovy*, 1988; *Garcia and Sassi*, 1999; *Garcia et al.*, 1997]. These tropical oscillations in turn contribute to the varia-

[1]Now at Institute for Chemistry and Dynamics of the Geosphere I, Forchungszentrum, Jülich, Germany.

[2]Now at High Altitude Observatory, National Center for Atmospheric Research, Boulder, Colorado, USA.

0148-0227/02/2001JD000577

bility of Kelvin waves [*Shiotani and Horinouchi*, 1993; *Canziani et al.*, 1995]. Where the waves encounter a critical level (westerly winds equal to wave phase speed), they will dissipate. This means, for example, that low frequency Kelvin waves rarely propagate to very high altitudes in the middle atmosphere because of the likelihood of encountering weak westerly winds due to the QBO or SAO [*Canziani and Holton*, 1998; *Canziani*, 1999]. Higher-frequency Kelvin waves can penetrate much further [*Hirota*, 1979; *Salby et al.*, 1984; *Riggin et al.*, 1997] and have been observed as high as the lower thermosphere.

[4] In addition to their contribution to dynamic variability, Kelvin waves affect the distributions of trace species by two mechanisms. First, the vertical velocity perturbations advect chemical species that have a significant vertical gradient and long photochemical lifetime. Second, temperature perturbations affect the production and loss rates due to the temperature dependence of reaction rates; this in turn can cause perturbations in the concentrations of short-lived species. *Randel* [1990] and *Salby et al.* [1990] showed observations of the variations of several species and compared these with theoretically predicted perturbations. In particular, strongest coherent Kelvin wave signals are found for trace species that have long lifetimes and sharp vertical gradients or have short lifetimes and equilibrium concentrations strongly dependent on temperature. Other studies have looked primarily at ozone in the middle and upper stratosphere [*Hirota et al.*, 1991; *Randel and Gille*, 1991; *Canziani et al.*, 1994] and found agreement with the theoretical prediction that the most important effect is the dependence of ozone photochemistry on temperature.

[5] Almost all of the global Kelvin wave temperature and trace species observations mentioned above were made using satellite observations that have good vertical resolution. This is important even in the upper stratosphere where the known Kelvin waves have relatively long vertical wavelengths ($\geq$10 km). Kelvin waves are not well resolved in the nadir-viewing satellites used for routine temperature monitoring of the stratosphere by National Center for Environmental Prediction. They have been detected in ozone column observations [*Ziemke and Stanford*, 1994] despite the limited vertical resolution inherent in these data. Other analyses have detected Kelvin waves with lower resolution data [*Hirota*, 1978], but such observations are rare. The Kelvin waves most commonly seen in the lower stratosphere have very short vertical wavelengths and are even more difficult to observe from satellite. In addition, they are suppressed during the westerly phase of the QBO. They have, however, been observed under favorable conditions by several instruments on the Upper Atmosphere Research Satellite (UARS). *Shiotani et al.* [1997] and *Canziani* [1999] found these waves in CLAES temperature data and *Srikanth and Ortland* [1998] saw them during September 1994 in both HRDI wind data and MLS temperature data.

[6] The observations described in this paper were made during the two flights of the Cryogenic Infrared Spectrometers and Telescopes for the Atmosphere (CRISTA). The data include temperatures and concentrations of a number of trace species. Profiles are inverted from three simultaneous limb-scanning telescopes and have high vertical and horizontal resolution. Each of the flights lasted for a little more than a week; they occurred during different times of the year and different phases of the QBO. Several Kelvin modes are clearly identified during each flight. Observed waves range in frequency from slow (periods $\geq$20 days) to very fast (periods around 3 days) and in altitude from the tropopause to the upper mesosphere.

[7] The focus of this study is determined by the strengths and limitations of the CRISTA data. The former include the high vertical and horizontal resolution, the broad vertical range of the profiles, and the simultaneous measurements of temperature and trace species. The primary limitations are the short duration of the two CRISTA flights and the irregular sampling. With these constraints, we look at details of the wave structure and how it evolves. We are able to determine variation of wave fields from day to day although, if their periods are long compared to the CRISTA mission, we can not always determine the wave periods exactly. Theoretical descriptions of Kelvin wave structure are used to confirm the presence of Kelvin waves.

[8] Section 2 gives a brief description of the data and analysis. Section 3 presents observations highlighting the Kelvin waves that were evident in the temperature fields. Section 4 discusses the relationship of the observed Kelvin waves with one another and with the background mean wind. Section 5 presents Kelvin wave signatures in the concentrations of five trace species in the stratosphere. Conclusions are given in section 6.

2. Description of Data and Analysis

2.1. CRISTA Instrument and Inversion

[9] CRISTA (Cryogenic Infrared Spectrometers and Telescopes for the Atmosphere) employs limb-scanning spectrometers designed to measure temperature and trace species in the middle atmosphere at high spatial resolution. CRISTA operates on board the Shuttle Pallet Satellite (SPAS), a free-flying satellite launched and retrieved by the Space Shuttle. CRISTA measures simultaneously with three telescopes whose viewing angles are offset by 18°. This gives a global data set with high horizontal and vertical resolution and a broad vertical range. A brief description of the instrument is given in the work of *Riese et al.* [1997]. Details of the instrument and inversion are contained in the studies of *Offermann et al.* [1999] and *Riese et al.* [1999].

[10] The first flight of CRISTA, hereafter CR-1, took place during early November 1994. Days of year 308–316 correspond to 4–12 November. The second CRISTA flight (CR-2) occurred in August 1997. Days of year 220–228 correspond to 8–16 August. This paper uses version 3 of the inverted data from CR-1 and version 1 from CR-2.

[11] A number of different operating modes were used during the CRISTA flights. *Riese et al.* [1999] and *Grossmann et al.* [2002] describe the modes and scheduling for CR-1 and CR-2, respectively. The data used in this study are from the M1 and M2 modes. The M1 mode extends from the tropopause to the upper mesosphere. M2 is nominally a stratospheric mode but every fourth scan (generating three temperature profiles) extends into the mesosphere.

[12] CRISTA stratospheric temperature profiles are inverted from CO_2 12.6 μm radiance. Reconstruction of the tangent height is supported by the accurate star tracker on board. The inversion uses an onion peeling technique. Tangent points of radiance data are separated 1.5 km in the vertical. For stability, the inversion of radiance to get temperature is performed separately on two profiles, each taking every other point (vertical spacing 3 km, offset by 1.5 km). These two profiles are then recombined to produce inverted temperature profiles at 1.5 km spacing. Temperature systematic and random errors at 40 km are 2.1 K and 0.4 K, respectively [*Riese et al.*, 1999]. Random temperature errors of the extended scans (see above) are a factor of 1.5 larger. Relative pressure is constructed from temperature with a tie-on in the lower stratosphere (23 km) to assimilated data from the Goddard Data Assimilation Office.

2.2. Data Processing

[13] Inversion of the CRISTA radiances yields vertical profiles that have variable altitude ranges and are on a variable grid based on the tangent points. The resulting horizontal distribution of profiles can be seen in, e.g., *Oberheide et al.* [2002]. All data were interpolated to fixed altitudes with 1 km spacing. The data are then used in two forms: binned in space and time, described in this subsection, and unbinned but analyzed by a fitting technique, described in the following subsection. The former analysis illustrates phase speed and daily variability of low frequency waves; the latter is able to isolate the structure of higher-frequency waves.

[14] The procedure for creating binned fields for CRISTA tropical data was, first, to separate the data by observing mode (M1 and M2) and by telescope (left, center or right). For each of these, a reference mean profile was created that was the average of all observations between 10°S and 10°N for all longitudes and times. Perturbation profiles were obtained from each profile by subtracting the appropriate reference mean. This separation by mode and telescope minimizes the impact that systematic difference might have on the perturbation fields [*Ern*, 2000] (M. Ern et al., Calibration procedures and correction of detector signal relaxations for the CRISTA infrared satellite instrument, submitted to *Applied Optics*, 2002). Because of the large number of profiles produced by CRISTA during a day, the bins contain many profiles (usually 50–100) that average out any remaining differences resulting from instrumental effects. In the binned data to be shown in section 3, perturbation data from each equatorial profile was put into a bin of 30° longitude and one day. Unless otherwise noted, all latitudes (10°S to 10°N) are averaged together.

[15] Where it makes sense physically, those binned data are used to illustrate the wave behavior during the CRISTA flights. The binning procedure allows us to see daily variations in the wave structure and irregularities in the phase that would not be resolved by analysis such as spectral decomposition. For example, the phase progression of a particular zonal wave number gives an estimate of the period, even if the period is longer than the data record. However, because of binning in time, the binned data can distort or obscure certain features such as the structure and behavior of short period waves.

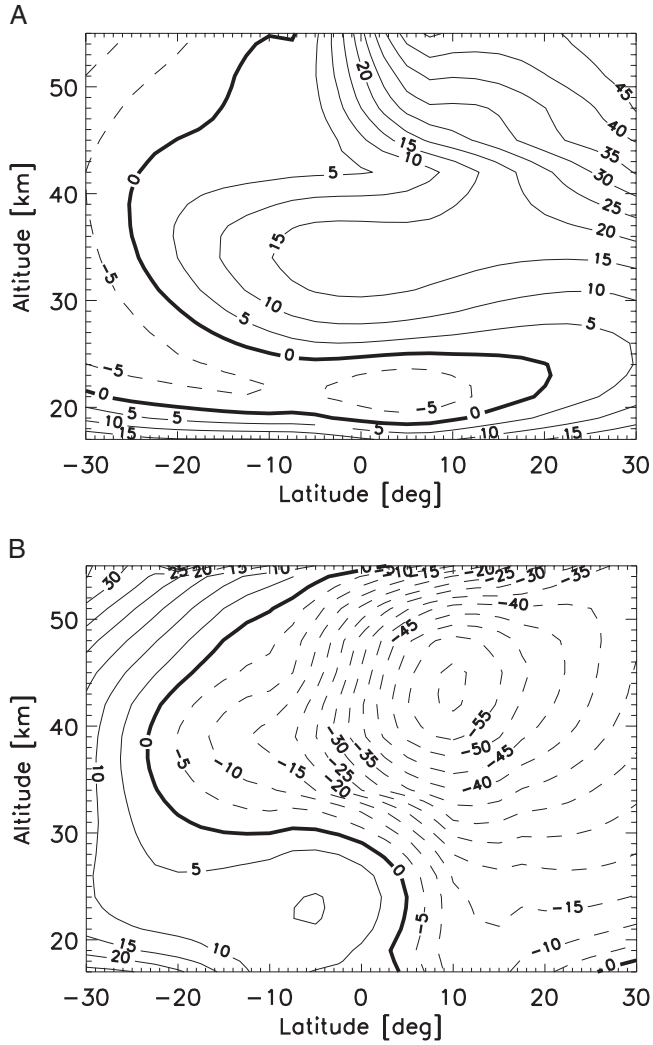

Figure 1. Zonal mean wind over the tropical region averaged over the entire mission for a) CR-1 and b) CR-2. Units are ms^{-1}.

2.3. Frequency Fitting

[16] To isolate particular traveling waves, we use a fitting function that follows from the assumed form of a traveling wave and is given by:

$$T_i' = A \sin(kx_i - \omega t_i + \phi) \quad (1)$$

where T_i', t_i and x_i are temperature deviation from the zonal mean, measurement time and longitude of an individual CRISTA measurement, respectively. The zero points in time are Day 310 and Day 222 for CR-1 and CR-2, respectively. The ground based frequency of the wave ω and the zonal wave number k are prescribed and the amplitude A and the phase ϕ are estimated by means of a least squares Fit (LSF) procedure. They are assumed to remain constant over the period of analysis.

[17] The wave number k takes only integer values (1, 2, 3,...) and is expected to remain the same over the domain and lifetime of the wave. The amplitude may vary as a wave packet grows and decays and as the wave prop-

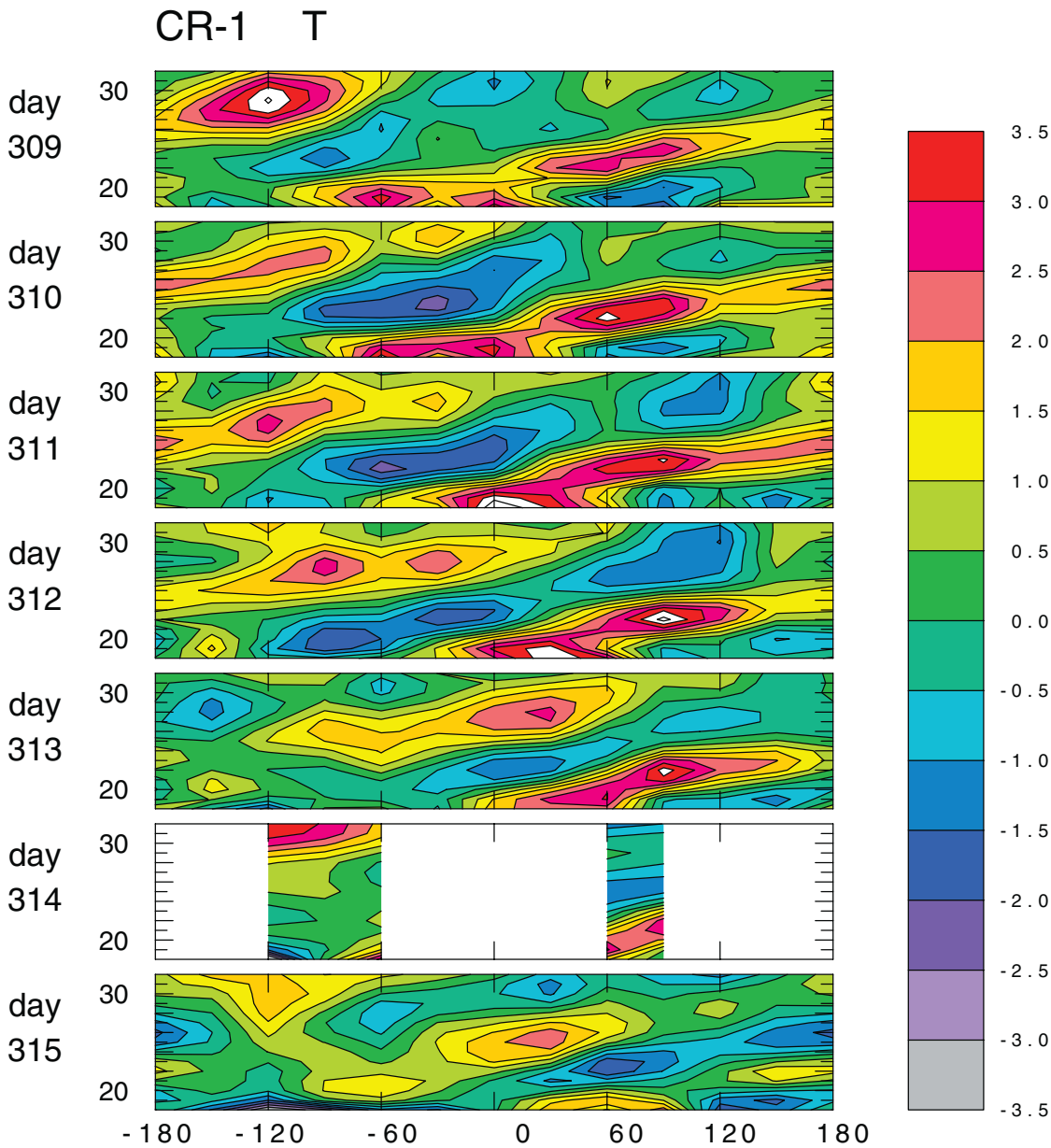

Figure 2. Longitude × altitude cross-sections of CR-1 temperature deviation from the mission mean, averaged over the latitude band 10°S to 10°N. Panels show a sequence of days. Vertical scale extends from 18 to 32 km. Units are K.

agates in a nonzero background wind. The frequency can change with altitude because of shear in the background zonal wind. We use several cross-checks to verify the wave frequencies identified in the LSF technique. First, for longer period waves ($\tau \geq 7$ days), we compare the frequency from the LSF analysis with that identified from a time-longitude plot of the phase progression of the temperature deviations. In addition, we calculate the percentage of standard deviation which is described by the fit. Because of the short duration of the CRISTA flights, the frequency fits are not orthogonal.

[18] To determine the limitations of the frequency fitting technique, we performed a number of tests on synthetic data. The tests look at cases where wave amplitude can vary with time, there can be more than one wave present simultaneously, realistic tidal temperatures are included, and the sampling is based on the actual CR-2 observation pattern. These indicate the following:

1. Temporal variations in amplitude degrade the reliability of the frequency analysis for waves with periods longer than 7 days.

2. The diurnal and semidiurnal tide can in general alias into other frequencies and/or wave numbers but do not make a significant contribution to any of the waves identified in this paper.

3. Although it is possible to verify that longer period waves are present (i.e., through the phase progression), the fitting technique alone is not able to distinguish the exact

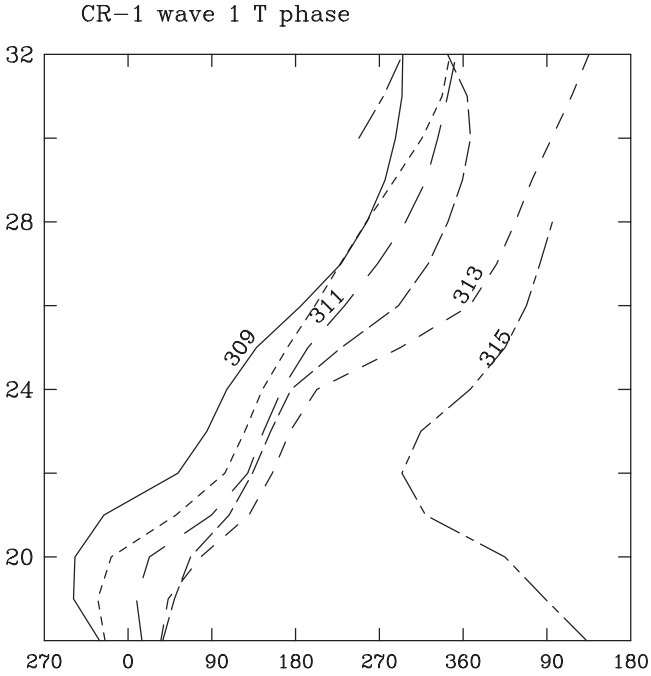

Figure 3. Phase of wave number 1 as a function of height on each of 6 days of the CR-1 mission. Phase is plotted only where amplitude exceeds 0.3 K. Labels refer to day of year; phase for day 314 is not shown because of insufficient data.

frequency for realistic nonsteady waves, particularly when more than one frequency is present.

4. The "beating" associated with the interference of two waves with the same zonal wave number but different frequencies and vertical wavelengths is difficult to disentangle if one of the wave periods exceeds 7 days.

With these findings in mind, we use caution in interpreting the analysis results. The frequency fitting analysis is used primarily for mapping out the structure of the waves. All waves presented here also show other evidence convincing us that they are likely to be Kelvin waves.

[19] Close inspection of the CR-2 wave patterns indicates an obvious change in the wave pattern during the course of the mission. Therefore an additional analysis of the second mission divides it into two parts that are analyzed separately.

3. Temperature Structure of Kelvin Waves

[20] The primary dynamical measurement of the CRISTA instrument is temperature. The high resolution of the CRISTA data permit a detailed look at the wave structure, while the short duration requires us to look at all the days individually. For understanding Kelvin wave propagation and structure, it is also important to know the background zonal mean wind in the equatorial region. Tropical zonal mean winds averaged over the two missions are shown in Figure 1. These have been derived from the CRISTA geopotential using the balance wind approximation and interpolated between 7.5°S and 7.5°N with a cubic spline interpolation. See *Oberheide et al.* [2002] for details.

[21] *Ward et al.* [1999] showed that the diurnal tide in temperature was quite large overall during the first CRISTA flight. In the upper stratosphere, the temperature tidal amplitude reached a local maximum of about 2 K and had a vertical wavelength of 28 km. During CR-2, the diurnal tide was weaker but there was, in addition, a nonmigrating tide with significant temperature amplitude [*Oberheide*, 2000]. Because of the short duration of the CRISTA flights, there is not much progression in local time. Tides will appear as almost stationary features. The impact of tides in the stratosphere is weak because of their small amplitudes there. Tests with synthetic data found that tidal contamination of the results is minimal even in the lower mesosphere.

3.1. Structure of Tropical Waves in CRISTA-1

[22] We will begin by showing the structure of the tropical waves that appear in CR-1 temperature. CR-1 took place in early November 1994. Figure 2 shows the perturbation temperature as a function of longitude and altitude in the lower stratosphere, averaged across the equator from 10°S to 10°N. The mean temperature has been subtracted to highlight the perturbation structures. From top to bottom, the panels show successive days. The most striking feature on this figure is the prominent wave number 1 structure with a strong eastward phase tilt with height. Looking more closely, one can also make out a wave 2 structure that is most pronounced in the lowest levels (18–22 km). These are the Kelvin waves that were clearly identified during the first CRISTA flight, and their structure will be discussed below. Although these waves have significant amplitude, their vertical wavelength is fairly short and they would

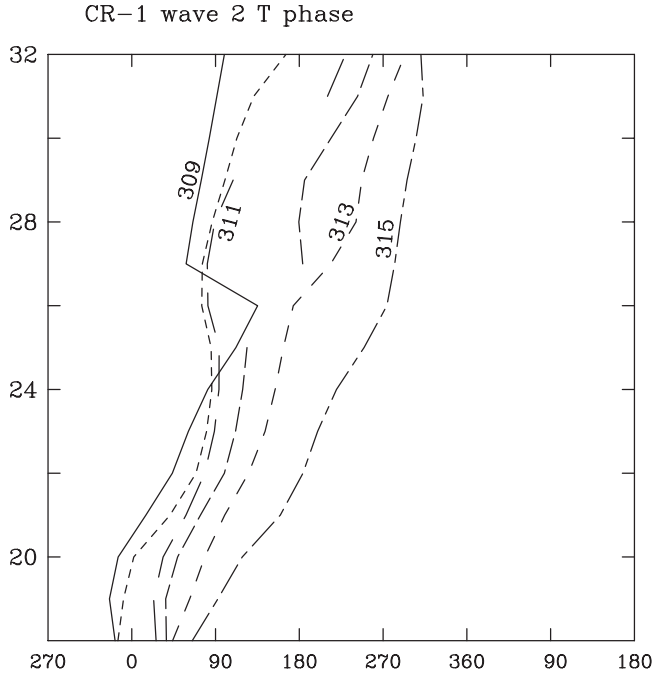

Figure 4. Phase of wave number 2 as a function of height on each of 6 days of the CR-1 mission. Phase is plotted only where amplitude exceeds 0.15 K. Labels refer to day of year; phase for day 314 is not shown because of insufficient data.

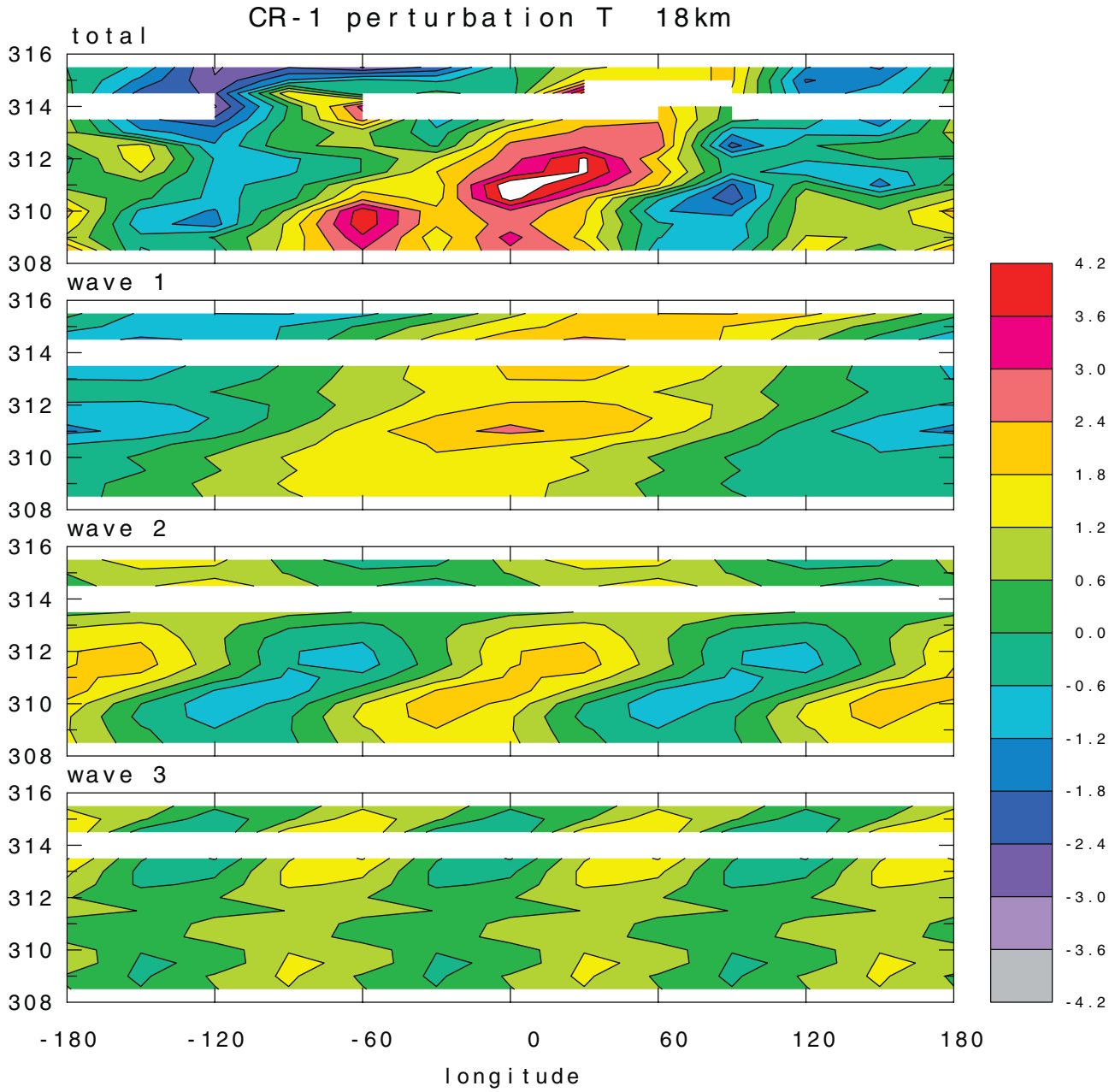

Figure 5. Longitude × time cross-sections of CR-1 temperature deviation from the mission mean at 18 km, averaged over the latitude band 10°S to 10°N. Top panel shows total; lower panels show contributions from wave numbers 1, 2 and 3, respectively.

therefore be difficult to detect in nadir-viewing satellite instruments; they do not have the structure of Kelvin waves in the NCEP analyses for this period.

[23] The temperature perturbations of Kelvin waves tilt eastward with height and move eastward with time. Figure 3 and Figure 4 show the daily phases of waves 1 and 2, respectively, in the stratosphere during CR-1. The phases are plotted only where the amplitudes exceed a threshold (0.3 K for wave number 1; 0.15 K for wave number 2). Note that there is a gap of one day due to insufficient data on day 314. Wave 1 shows a very slow eastward phase progression in the lower stratosphere and a faster phase progression between 25 and 30 km; there is no clear wave progression above 32 km. On most days, the amplitude of the wave is above the threshold at all altitudes and the phase of the wave varies continuously between the two phase regimes. Wave 2 also shows a slow phase progression in the lower stratosphere (18–25 km) and a more rapid phase progression above.

[24] There is, in addition, a wave 3 perturbation that appears to have a slowly eastward moving phase just at the tropopause, although no vertical structure information is available because the amplitude decays by 20 km. The behavior of wave 3 can be seen in Figure 5, which shows the temperature perturbation at 18 km and the contributions of wave numbers 1–3 to the total perturbation. The simul-

taneous appearance of these three different wave numbers suggests that a packet of waves were excited and that they were able propagate to different altitudes. A similar pattern was seen by *Salby et al.* [1984] for wave numbers 1 and 2.

[25] With the short data record, a precise separation is not possible but the appearance from Figures 3 and 4 is that there are discontinuities between two waves with different frequencies and vertical structures. Previous observations have suggested that middle atmosphere Kelvin waves are grouped into three, or possibly four, different frequency ranges. The slow Kelvin waves [*Wallace and Kousky*, 1968; *Shiotani et al.*, 1997] have periods of 10–20 days and are seen in the lower stratosphere. The fast Kelvin waves [*Hirota*, 1978, 1979; *Hitchman and Leovy*, 1988] have periods of 6–10 days and are more evident in the middle to upper stratosphere. The ultrafast Kelvin waves [*Salby et al.*, 1984; *Lieberman and Riggin*, 1997], with periods of 3–4 days, are seen in the upper stratosphere, mesosphere and lower thermosphere. There is also evidence of waves in an ultraslow frequency range (periods 25–30 days) in the lowest part of the tropical stratosphere [*Canziani*, 1999]. Observations in which more than one frequency range has been observed simultaneously indicate that there appear to be discrete preferred frequency ranges with a clear separation between them [*Salby et al.*, 1984; *Canziani et al.*, 1994; *Shiotani et al.*, 1997].

[26] The consistent eastward-tilting phase structure characteristic of a Kelvin wave in CR-1 disappears above about 30 km. However, previous observations have shown that Kelvin waves that are observed in the upper stratosphere are either "fast" or "ultrafast". High frequency Kelvin waves (periods of $\lesssim$6 days), if present, would be distorted or masked by the daily binning used for creating Figures 2, 3, 4, and 5. The fitting procedure described in section 2 can detect signals from high frequency waves. Results from this analysis for a large range of periods down to one day were screened but also did not reveal any sign of coherent, equatorially trapped eastward traveling wave activity in the mesosphere or upper stratosphere during CR-1.

[27] The wave number 1 and 2 temperature perturbations described above have been referred to as Kelvin waves. They have several of the basic Kelvin wave characteristics: significant amplitude in the equatorial region, eastward phase tilt with height, and eastward progression with time. We compare additional details of the wave structures to those of a theoretical Kelvin wave to verify the Kelvin wave identification.

[28] Another characteristic that can be used to identify Kelvin waves is the relationship between frequency ω, zonal wave number k and vertical wave number m, which is known as the dispersion relation. If the background wind shear is weak, as it was during the CR-1 mission, the dispersion relation takes on the simple form

$$\omega - k\bar{u} = \frac{-Nk}{m} \tag{2}$$

where N is the buoyancy frequency and u is the average zonal wind. For a given wave number, higher-frequency waves will have larger vertical wavelengths. There are two distinct frequencies of wave number 1. For a narrow region in the lower stratosphere (20–24 km), the phase progression is about 21 deg/day (86° from day 309 to day 313 at 22 km), in the slow to ultraslow range. The background zonal wind, which shifts from 5 m/s westerly to 5 m/s easterly, gives a Doppler shifted phase speed ranging from 17 to 25 deg/day. This implies a vertical wavelength of 7–10 km. At 28 km, the apparent frequency is higher (34 deg/day) but the background wind is again westerly and the Doppler shifted frequency is about 30 deg/day (vertical wavelength of 12 km). There is also a change in the vertical structure of wave number 1 in the lower stratosphere; the vertical wavelength is smallest at altitudes between 20 and 22 km and becomes longer above. As noted, some but not all of the change can be accounted for by the shift in background wind. Assuming vertical and zonal wavelength and intrinsic frequency are fixed wave characteristics, one would interpret the observations as indicating that there is more than one wave present. For wave 2, the apparent frequencies are about 20 deg/day at 22 km (vertical wavelength of 8 km) and 37 deg/day above 26 km (vertical wavelength of 15 km) and, again, it appears as if more than one wave is present.

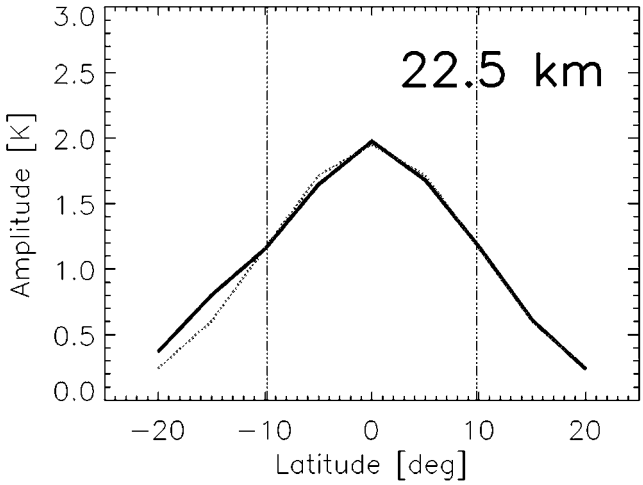

Figure 6. Latitude structure of CR-1 wave number 1 temperature at 25.5 km, based on the frequency fitting for a period of 12 days (solid line). Also shown is a Gaussian fit centered on the equator (dashed line) corresponding to a Kelvin wave 1 with an 11-day period. Units are K.

[29] Kelvin wave amplitudes are symmetric about the equator with maxima near the equator. A slight offset can occur in the presence of meridional shear in the background zonal wind [*Boyd*, 1978]. For an idealized Kelvin wave, the latitudinal structure is given by

$$T(y) = T_0 \exp\left[\frac{-\beta k y^2}{2(\omega - ku)}\right] \tag{3}$$

where T is temperature, y is latitude, and β is the meridional derivative of the Coriolis parameter. Figure 6 shows the CR-1 wave 1 amplitude as a function of latitude at 25. km. To generate Figure 6, we use the frequency fit

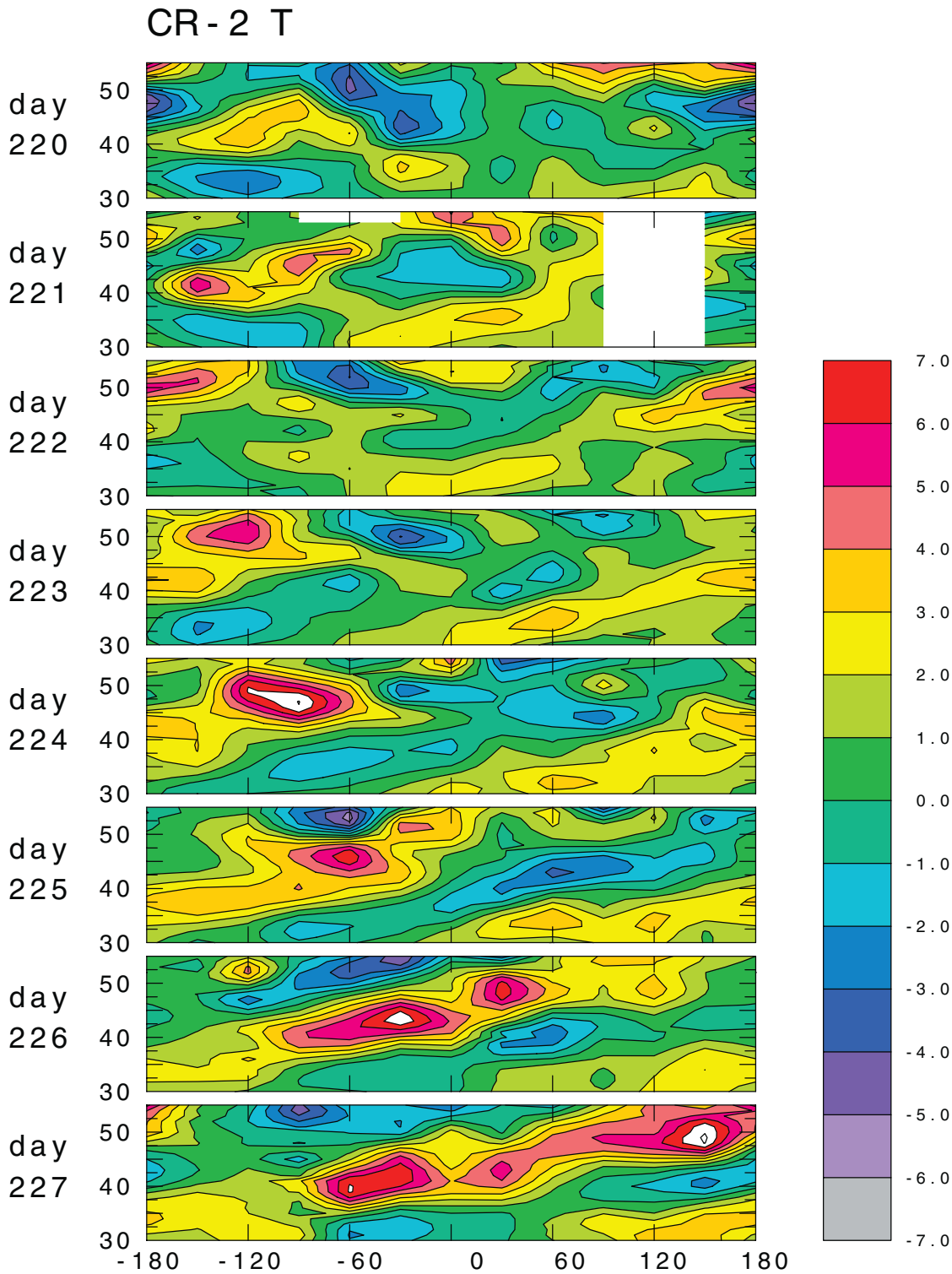

Figure 7. Longitude × altitude cross-sections of CR-2 temperature deviation from the mission mean, averaged over the latitude band 10°S to 10°N. Panels show a sequence of days. The altitude range is 30–55 km. Units are K.

information, described in section 2. For determination of the latitudinal structure of the observed waves, we use data binned in 5° latitude intervals over the entire mission. A Gaussian fit is also shown; the corresponding period is about 11 days. The correspondence in the shapes of the curves is excellent. The phase of this wave 1 (not shown) has almost no variation with latitude, as expected for a Kelvin wave.

3.2. Structure of Tropical Waves in CRISTA-2

[30] There are significant differences in the Kelvin waves that appeared during the first and second CRISTA flights.

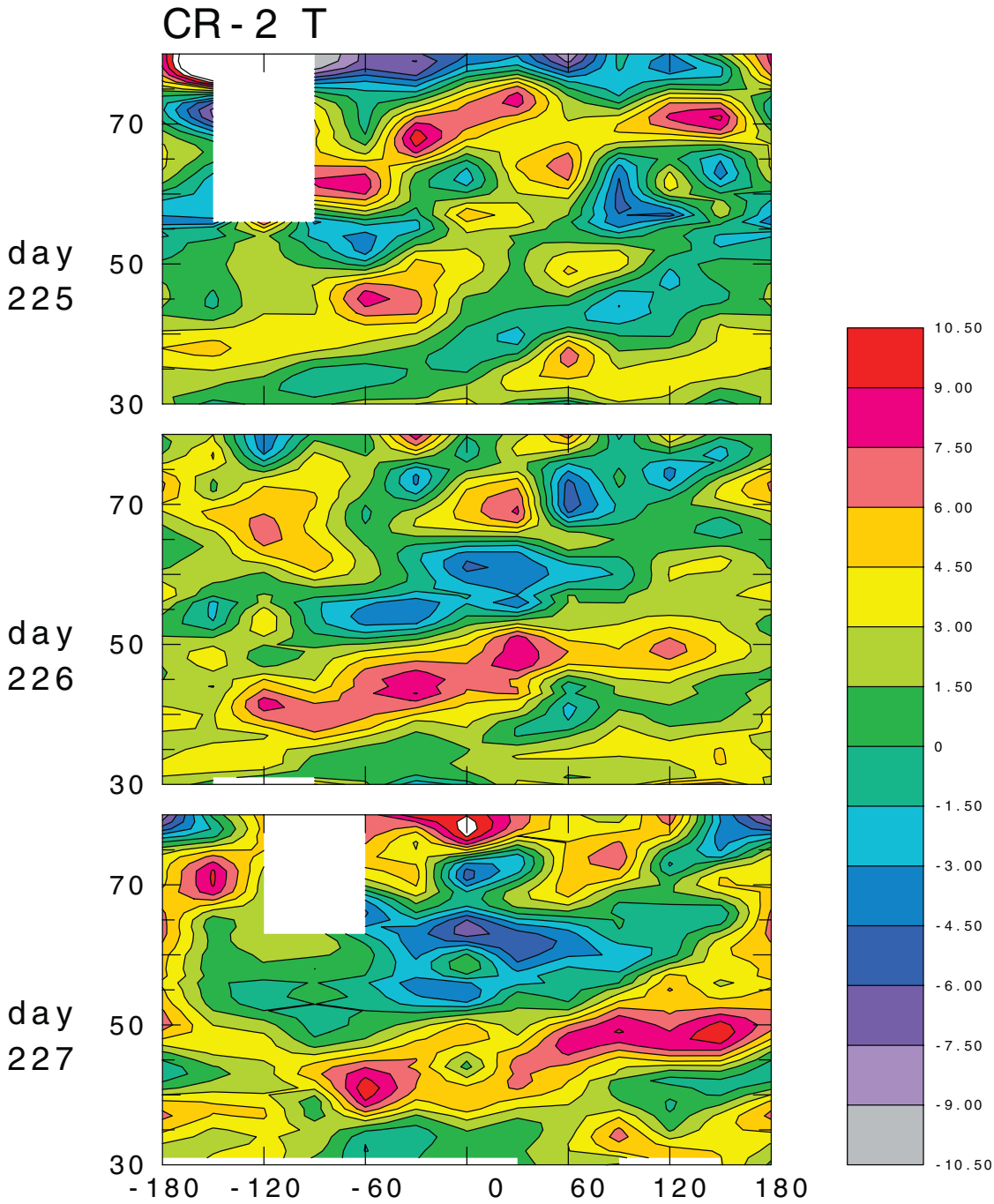

Figure 8. Longitude × altitude cross-sections of CR-2 temperature deviation from the mission mean, averaged over the latitude band 10°S to 10°N for days 225–227 over an altitude range from 30 to 80 km. Units are K.

This is due at least in part to the fact that the background zonal winds were different, associated with different phases of the QBO and SAO. During August 1997, the QBO was westerly through the entire lower stratosphere, eliminating the possibility of low-frequency Kelvin waves in the middle atmosphere. No identifiable Kelvin waves were found below 25 km. The SAO was in transition from easterly to westerly but still had significant easterly winds. During this mission, Kelvin waves were evident from the middle stratosphere to the upper mesosphere. Unfortunately, coverage of the higher altitudes (above 55 km) is intermittent so only limited information about the wave structure in the middle and upper mesosphere is available. Figure 7 shows the daily equatorially averaged temperature perturbations for the middle and upper stratosphere, with an eastward-tilting wave beginning to appear on day 221 and becoming large in the later days of the mission. During the last three days, coverage in the mesospheric mode was sufficient to extend this view to higher altitudes. Figure 8 shows the perturbation temperature structure over a wide vertical range (30 to

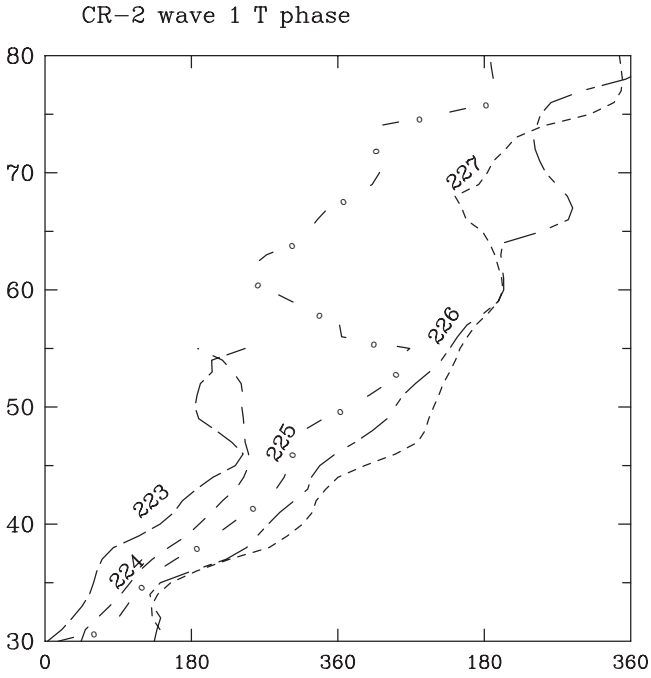

Figure 9. Phase of wave number 1 as a function of height on the last 5 days of the CR-2 mission.

80 km) for these three days. Although the eastward propagating wave has fairly large amplitude in the mesosphere, the perturbation field appears quite noisy compared with the large amplitude waves seen in the stratosphere. A number of small scale and/or rapidly changing processes in the mesosphere such as gravity wave breaking, inertial instability and tidal variability contribute to the higher spatial and temporal variability normally found there.

[31] The phase progression of wave 1 during days 223–227 of CR-2 is shown in Figure 9. (The phase tilt was westward with height during days 220 and 222; there is insufficient data for a determination of the wave structure on day 221.) Beginning on day 223, there is a clear eastward phase tilt and eastward phase progression. On the last two days the phase structure indicates a coherent pattern up to 70 km (see also Figure 8). In general, wave activity was more developed during the second half of the CR-2 mission and was, in addition, observed over a broader vertical domain because of the use of the mesospheric measuring mode. For this reason, some of the analysis described here was applied separately on the time periods day 220–223 (first half) and 224–227 (second half).

[32] A look at Figure 7 provides evidence that a large part of the temperature variability is associated with an eastward traveling wave number 1 disturbance. As noted above, the phase shift with time appears to be more rapid above 35 km than it is below there. This case differs from that seen in CR-1 in that, as described below, there is evidence for the existence of a high frequency wave 1 Kelvin wave (period about 4 days). With this being the case, the shift in phase speed apparent in Figure 9 can come from either or a combination of different physical situations.

1. The phase speeds seen on the figure represent the actual wave frequencies, which cover a wide range and vary with altitude.

2. The interference between a low frequency wave 1 with a short vertical wavelength and a higher-frequency wave 1 with a long vertical wavelength gives rise to an apparent continuous shift in phase speeds.

[33] Figure 10 illustrates the results of the frequency fitting technique using data from the second half of CR-2. The amplitude is indicated for a range of periods at all stratospheric altitudes. This again emphasizes the range of apparent periods. Two maxima appear. There is a weak maximum of 2 K near 34 km that has a period around 10–15 days. The other broad maximum amplitude ($\geq$3 *K*) extends from 40 to 50 km and covers a range of periods from 4 to 12 days. Clearly more analysis is needed to distinguish which wave frequencies are most likely to have contributed to the observed wave number 1. To do this, we take advantage of the fact that the frequency fitting technique is most reliable for short-period waves. In addition, we use the Kelvin wave dispersion relation and latitudinal structure equation to cross-check our interpretation.

[34] The analysis shows a robust 4 day wave 1 with maximum amplitude of 3.5 K at the equator between 45 and 50 km (Figure 11). The vertical phase tilt indicates a phase progression of 70° between the altitudes of 40 and 54 km at the equator, indicating a vertical wavelength of 36 km. This is close to the theoretical prediction of 42 km for a 4-day wave in a background wind of -20 m s^{-1} (see Figure 1). There is almost no phase shift with latitude across the equatorial region. The latitudinal variation of amplitude, shown in Figure 12, likewise corresponds very well with that predicted for a wave with this Doppler shifted period. Tests with synthetic data show that waves with periods shorter than the CRISTA mission but longer than 24 hours are well resolved. While there could in principle be contamination by other wave or tidal modes, there is no evidence of the presence of the components that would map into this particular wave number-frequency combination. The frequency fitting analysis for a 4-day wave 1 is therefore considered to be reliable.

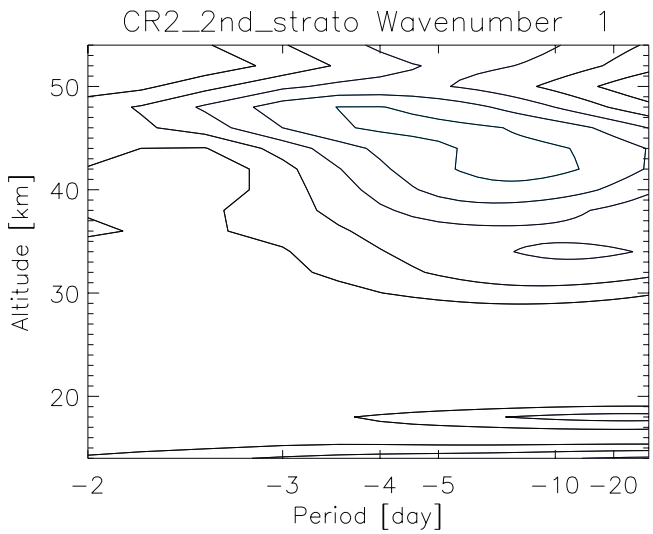

Figure 10. Amplitude of wave 1 from the frequency fitting for the second half of the CR-2 mission as a function of altitude and period. Contours are from 1 to 3 K at 0.5 K intervals.

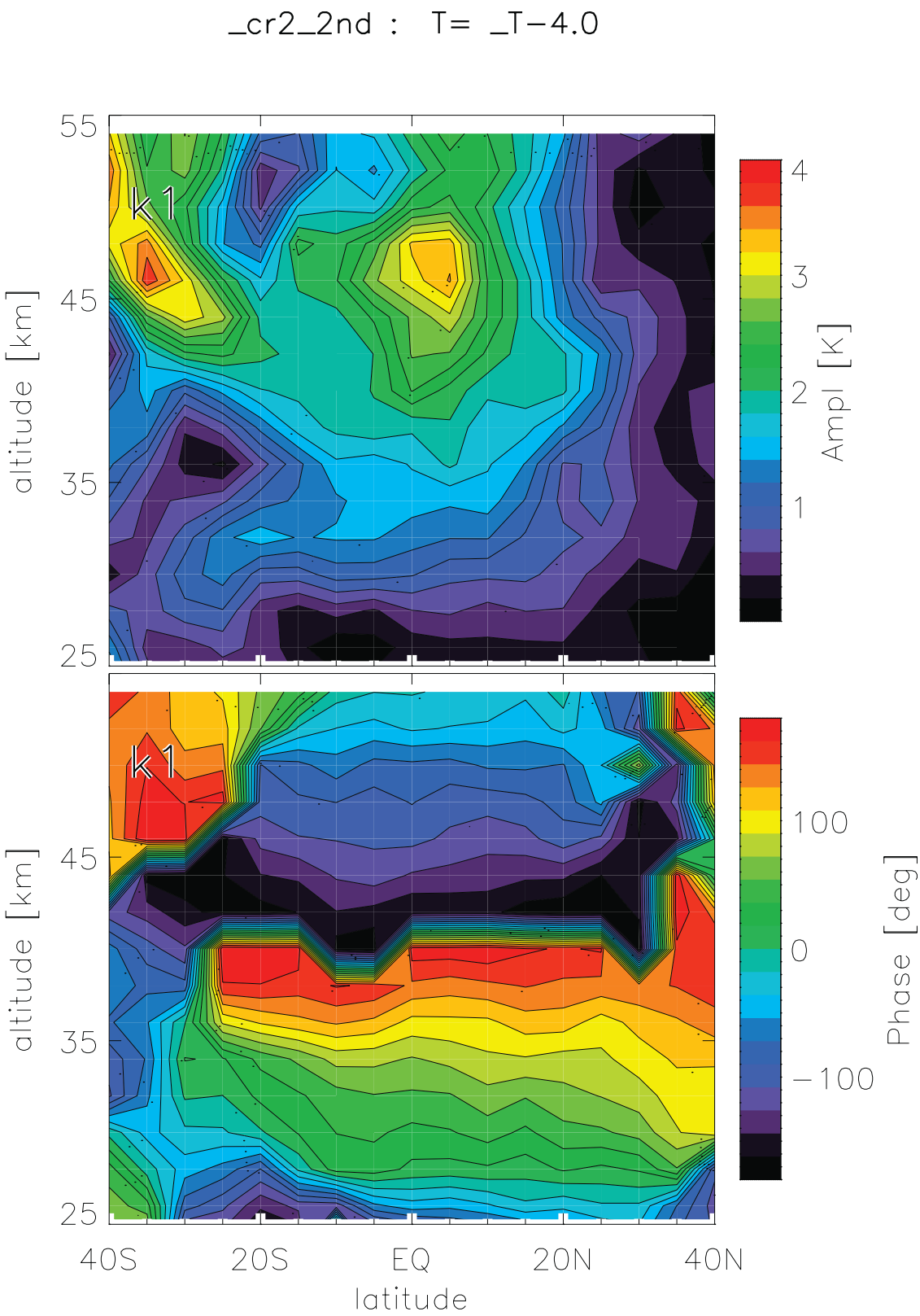

Figure 11. Wave number 1 from data fit to a structure with constant amplitude and a period of 4 days. Top panel shows amplitude and bottom panel shows phase. Fit is based on temperature data from the second half of CR-2.

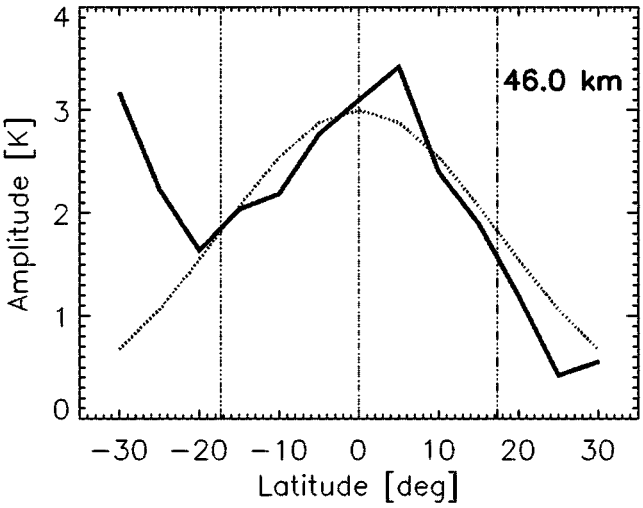

Figure 12. Latitude structure of CR-2 wave number 1 temperature at 46 km, based on the frequency fitting for a period of 4 days (solid line). Also shown is the idealized structure for a wave with this Doppler-shifted period (dashed line). Units are K.

[35] It appears from Figures 7, 8, and 9 that there is also a lower-frequency wave present. The period of 13 days in the middle stratosphere can be estimated from Figure 9; the fitting analysis with a period of 13 days (Figure 13) indicates that this component has significant amplitude over the range 30–45 km. It was also evident from Figure 10 that the longer period wave components tend to be dominant at lower altitudes than the shorter periods. The predicted vertical wavelength for a 13-day wave number 1 ranges from 5 km for a -20 m s^{-1} background wind to 11 km for zero background wind. The vertical wavelength determined from the analysis (see Figure 9 and Figure 13) is fairly short (10–20 km) around the altitudes of 30–40 km but still is at the upper limit (zero wind approximation) of the theoretical prediction. The lack of phase shift with latitude conforms to the predicted behavior. The latitudinal width of the amplitude estimated from the analysis is significantly wider than that predicted from Kelvin wave theory. In both cases (latitudinal width and vertical structure), the apparent structure of the wave is Kelvin-like but is characteristic of a shorter period than the 13-days identified from the observed phase progression. Tests show that superposition of two $k = 1$ waves with different periods will produce a perturbation temperature whose amplitude fits a Gaussian shape in latitude that is intermediate between the widths of the those for the two waves separately. Therefore, while there is evidence that a wave exists, the short span of the observations do not allow us to cleanly separate this wave from the shorter-period wave (or waves) that is also present.

[36] The frequency fitting analysis also reveals evidence for two high frequency waves with higher zonal wave number, both of which have structures that correspond well with theoretical Kelvin waves. There is a wave number 2 (illustrated in Figure 14) with a period of 3.5 days that is strong during the first half of the mission but was negligibly small in the second half. Wave number 2 is the dominant zonal wave number during days 220–223 in the altitude range 45–55 km and its eastward phase progression is clearly visible in longitude $\times$ time cross-sections (not shown). The vertical phase progression indicates a vertical wavelength of 28 km, almost identical to the theoretical prediction of 27 km. The latitudinal width for the wave is predicted to be 17.5° and the fit to the data give a best fit for 16.5°. All evidence supports the identification of this feature as a Kelvin wave. This particular periodicity has also been detected in tropical airglow variations [*Takahashi et al.*, 2002].

[37] There was also a small but coherent 5 day wave with an unusual zonal wave number of 4 that appears between 35 and 50 km during the second half of the mission (illustrated in Figure 15). The tests with synthetic data do not give any indication that such a signal would result from aliasing of any of the other waves observed during CR-2. Other evidence supports our conclusion that this feature is actually a Kelvin waves. The vertical wavelength inferred from the phase structure (18 km) corresponds well with that predicted by the dispersion relation with a mean wind of 20 m s^{-1}. The coefficients for the Gaussian structure in latitude cluster around 17° (close to that predicted from theory). Temperature and zonal wind perturbations that appear to be a Kelvin wave with zonal wave number 4 and a 5-day period have also been seen in lower stratospheric radiosondes by *Holton et al.* [2001].

4. Discussion of Wave Characteristics and Variability

[38] One of the intriguing aspects of the waves observed by CRISTA, as well as waves reported in other data, is the simultaneous appearance of several wave numbers and several frequencies. In this section, we describe the aspects of the observations relating to the relationship of different Kelvin waves to one another and to the background mean flow. Since the CRISTA flights were short, we cannot get a sense of the climatology of the waves. However, the high resolution of the data allow us to get a detailed snapshot of the diversity of Kelvin wave activity during two quite different periods.

[39] Zonal mean tropical winds for the two missions differed markedly, as shown in Figure 1. During November 1994, the QBO was in transition, with easterly winds below about 25 km and westerly winds above. The SAO still had westerly winds in the upper stratosphere. This means that very slow-moving Kelvin waves would encounter a critical line somewhere in the lower stratosphere, 25–30 km, while faster moving waves might be able to propagate to the middle or upper stratosphere. Because of the phase of the SAO, it is unlikely that there would be any but high frequency Kelvin waves that could propagate beyond the upper stratosphere.

[40] The background wind conditions are qualitatively consistent with the suite of waves seen in the CRISTA data. We have already noted one feature of the relationship between the waves observed: the shift from lower to higher frequencies for both waves 1 and 2. This occurred for both the lower stratospheric waves observed in CR-1 and the upper stratosphere and mesosphere wave number 1 observed during CR-2. Note also that the phase speeds of

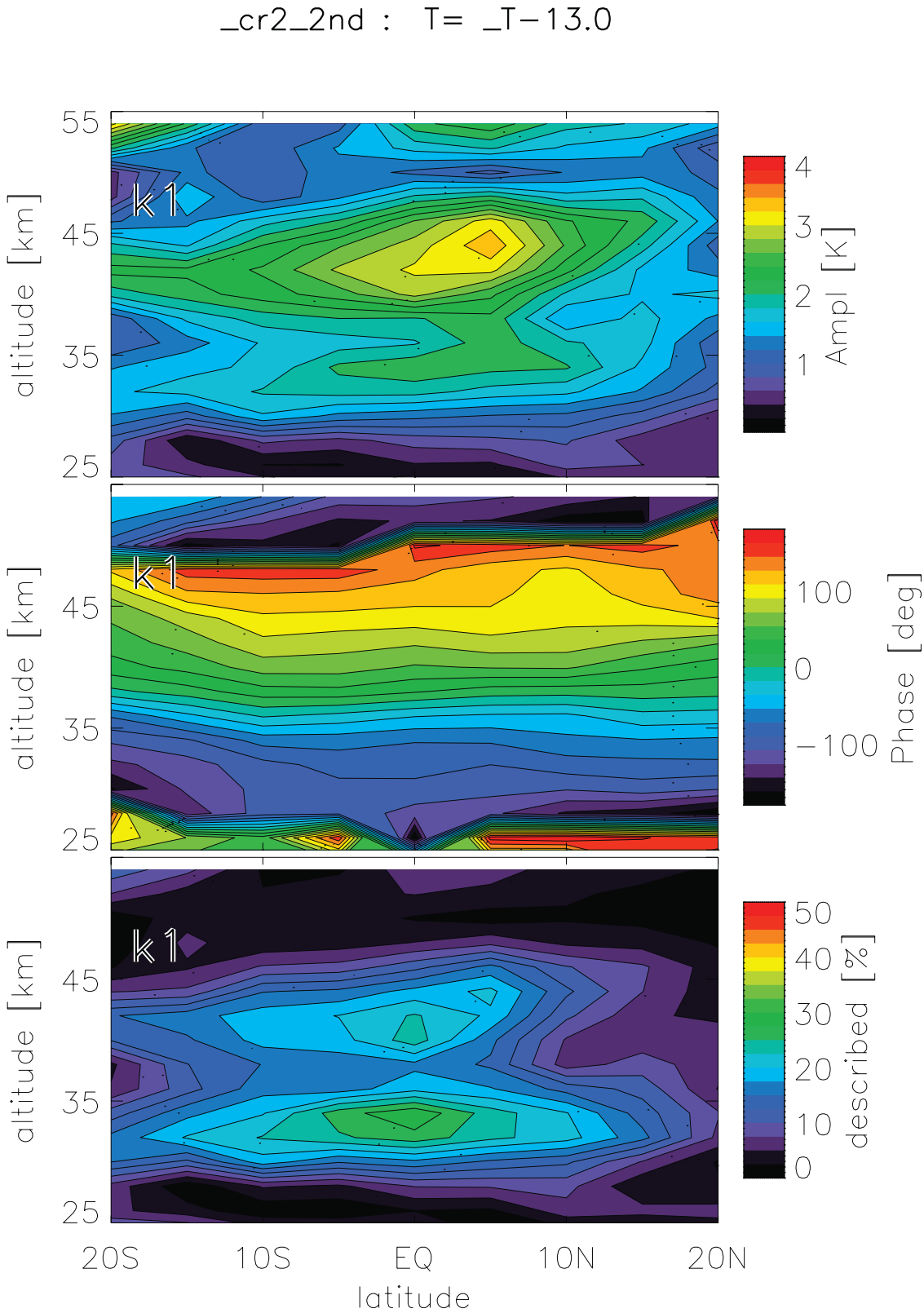

Figure 13. Wave number 1 from data fit to a structure with constant amplitude and a period of 13 days. Top panel shows amplitude, middle panel shows phase and bottom shows percent of standard deviation explained by the fitted wave. Fit is based on temperature data from the second half of CR-2.

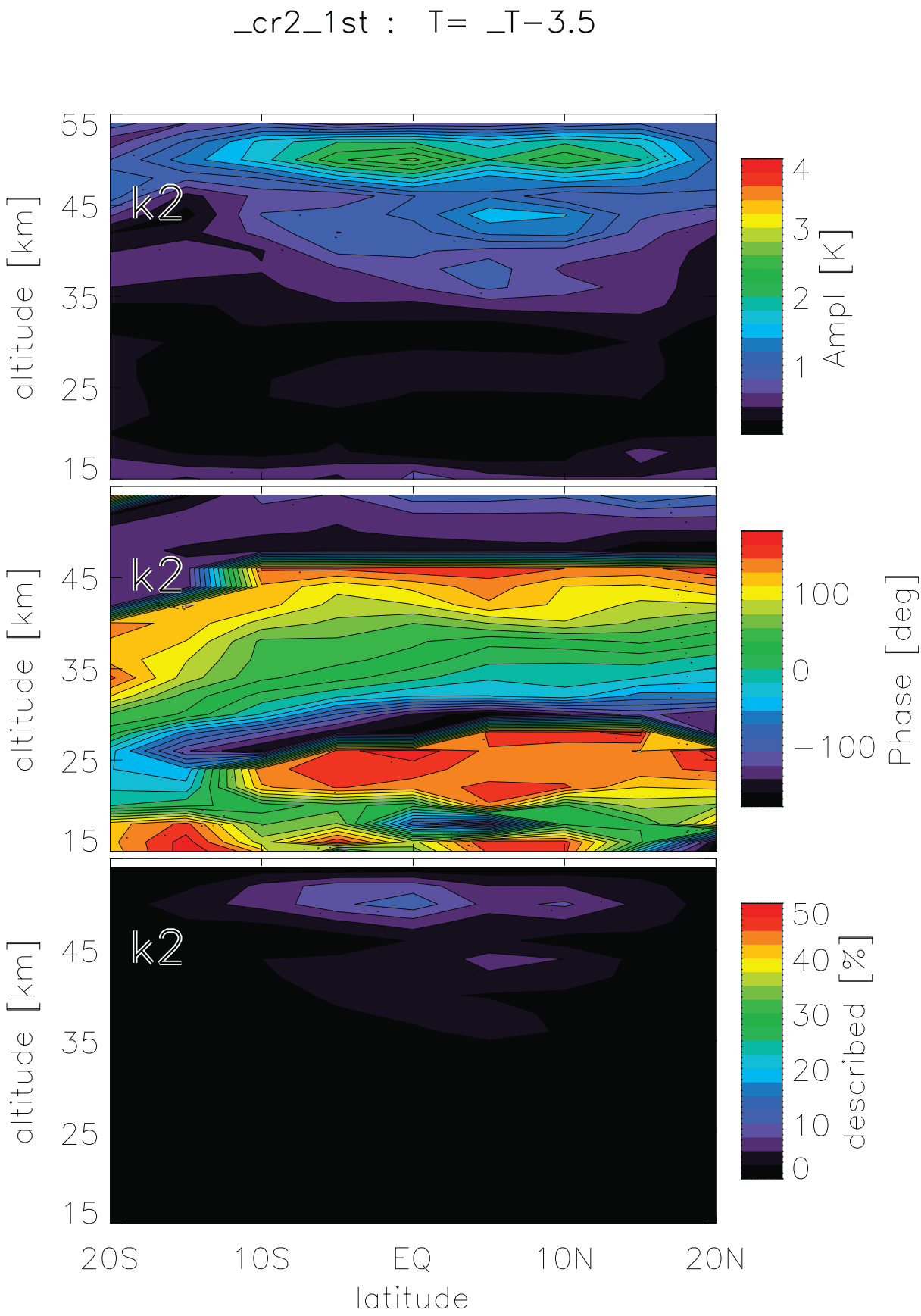

Figure 14. As in Figure 11, but for wave number 2, 3.5 day period during the first half of CR-2.

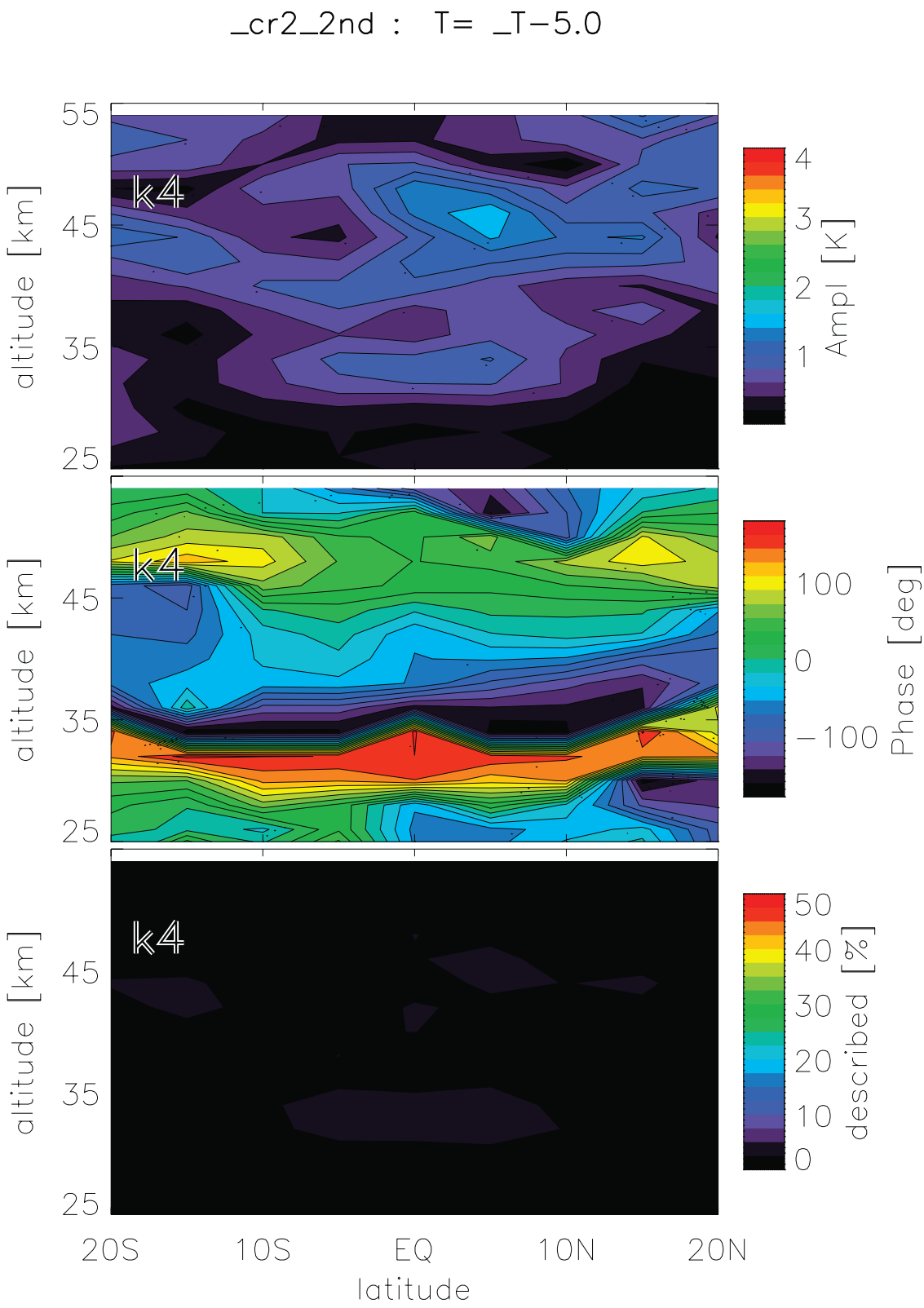

Figure 15. As in Figure 11, but for wave number 4, 5 day period.

wave 1 and 2 during CR-1 are similar. In the lowest part of the stratosphere both are around 15–20 deg/day and above 25 km both are about 35 deg/day. *Salby et al.* [1984], *Canziani et al.* [1994] and *Canziani* [1999] noted a tendency for simultaneous wave number 1 and 2 having similar phase speeds. *Holton et al.* [2001] found perturbations consistent with zonal wave numbers 2 and 4 with approximately the same phase speed. These give support for the

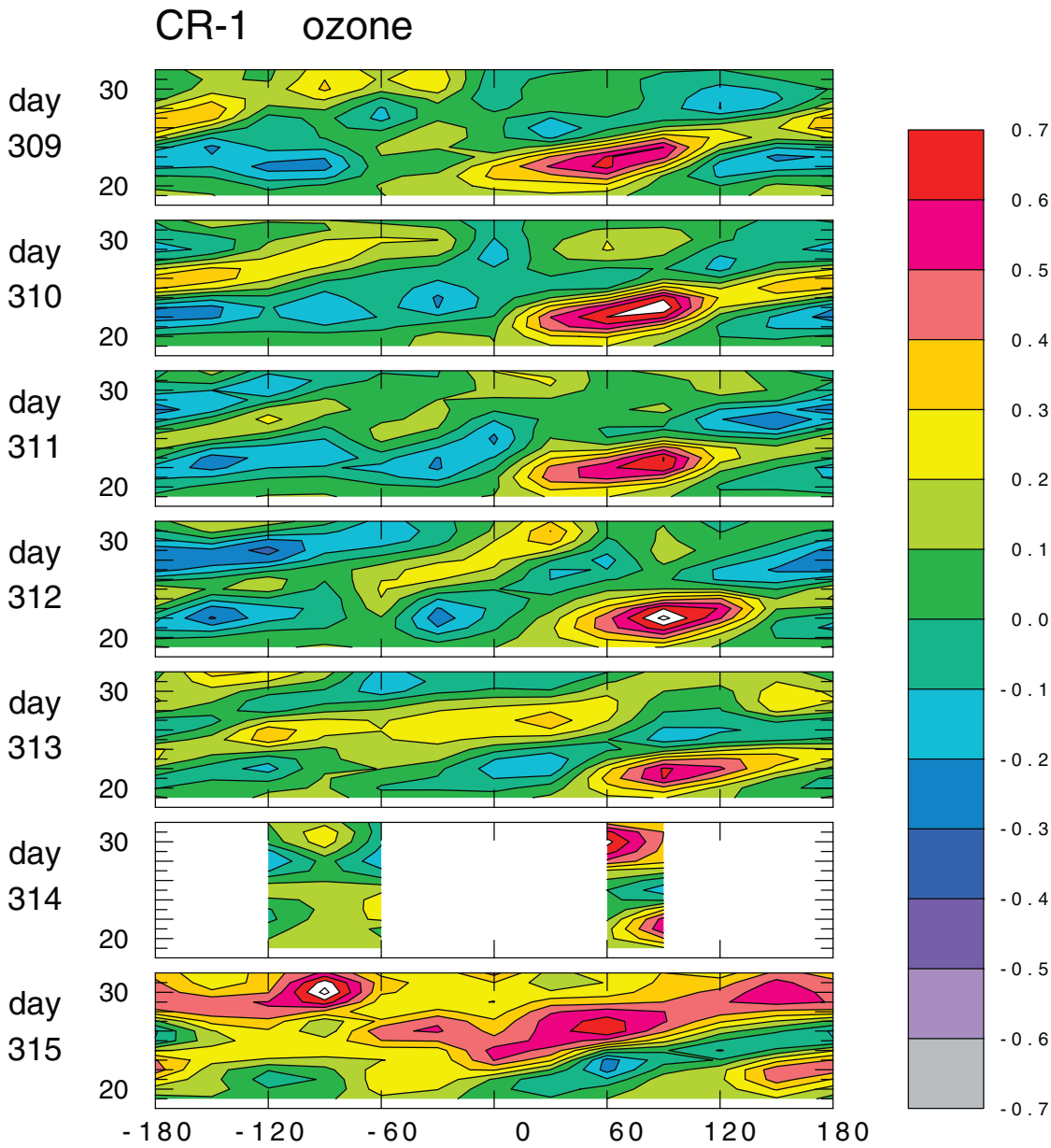

Figure 16. Longitude × altitude cross-sections of CR-1 O_3 mixing ratio deviation from the mission mean, averaged over the latitude band 10°S to 10°N. Panels show a sequence of days. Units are ppmv.

hypothesis that a distinct synoptic event has spawned a set of waves with different zonal harmonics.

[41] Several studies have looked at the pattern of tropical waves in the middle atmosphere that emanate from a tropospheric source [*Coy and Hitchman*, 1984; *Garcia and Salby*, 1987; *Salby and Garcia*, 1987]. A continuous range of frequencies can be generated by a discrete event. Dispersion will cause different frequencies to propagate vertically at different rates. However, the modeling studies do not explain why there is an abrupt change in the frequency with altitude rather than a continuous transition. The theoretical and modeling work found no such clean separation in the different frequency regimes.

[42] The CR-1 flight in early November occurred after the peak in the westerly phase of the stratopause SAO but was still in a regime characterized by significant westerly winds in the upper stratosphere. During CR-1, there were large disturbances in the tropical lower mesosphere although these did not appear to fit the description of Kelvin waves. In particular, phases did not tilt eastward with height and did not appear to move regularly between days. The wavelike structures appeared to be associated with inertial instability circulation cells identified in the stratopause region previously [*Smith and Riese*, 1999]. No evidence for fast or ultrafast Kelvin waves was found.

[43] CR-2 occurred in early August when zonal winds near the tropical stratopause were strongly easterly. The westerly (QBO) winds in the lower stratosphere prohibit the propagation of low frequency Kelvin waves but allow higher-frequency waves to penetrate. A number of tropical waves are found that appear to be Kelvin waves. Wave

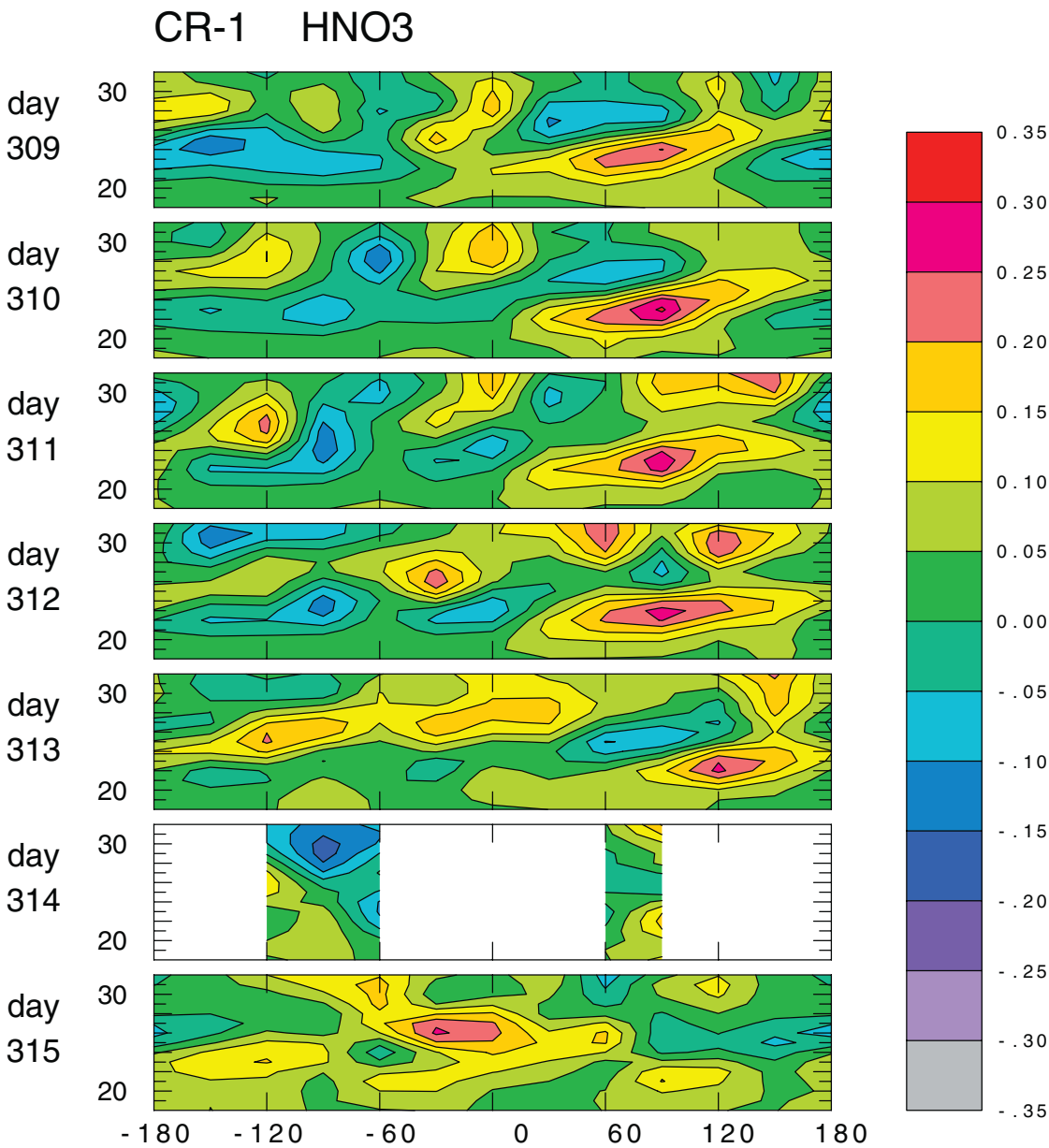

Figure 17. Longitude × altitude cross-sections of CR-1 HNO_3 mixing ratio deviation from the mission mean, averaged over the latitude band 10°S to 10°N. Panels show a sequence of days. Units are ppbv.

number 1, having different frequencies at different altitudes, dominates the equatorial perturbation temperature throughout the middle atmosphere. Weak ultrafast waves that fit all the characteristics of Kelvin waves were detected in the lower mesosphere. One noteworthy wave is a wave number 4, which is higher than is normally reported for Kelvin waves.

5. Kelvin Wave Signatures in Chemical Fields

[44] *Randel* [1990] showed that Kelvin waves will also have signatures in the concentrations of both long-lived and short-lived trace species. Other studies [*Randel and Gille*, 1991; *Hirota et al*, 1991; *Canziani*, 1994] have provided additional documentation of the impact that Kelvin waves have on ozone.

[45] It is noteworthy that, up until now, no signs of the low frequency Kelvin waves that occur in the lower stratosphere during the easterly phase of the QBO have been detected in satellite tracer fields. This includes the study of *Shiotani et al.* [1997] using CLAES data, which found strong signals of these lower stratospheric Kelvin waves in the temperature fields but none in ozone or water. Another instrument that had sufficient resolution in the lower stratosphere (LIMS) operated during the westerly phase of the QBO when these low frequency waves were absent. CR-1 results indicate that Kelvin waves do have a significant impact on the variations of lower stratospheric tracers and that these variations are closely linked to those of temperature, as predicted by theory. It is not clear why such variations were not apparent in the CLAES data.

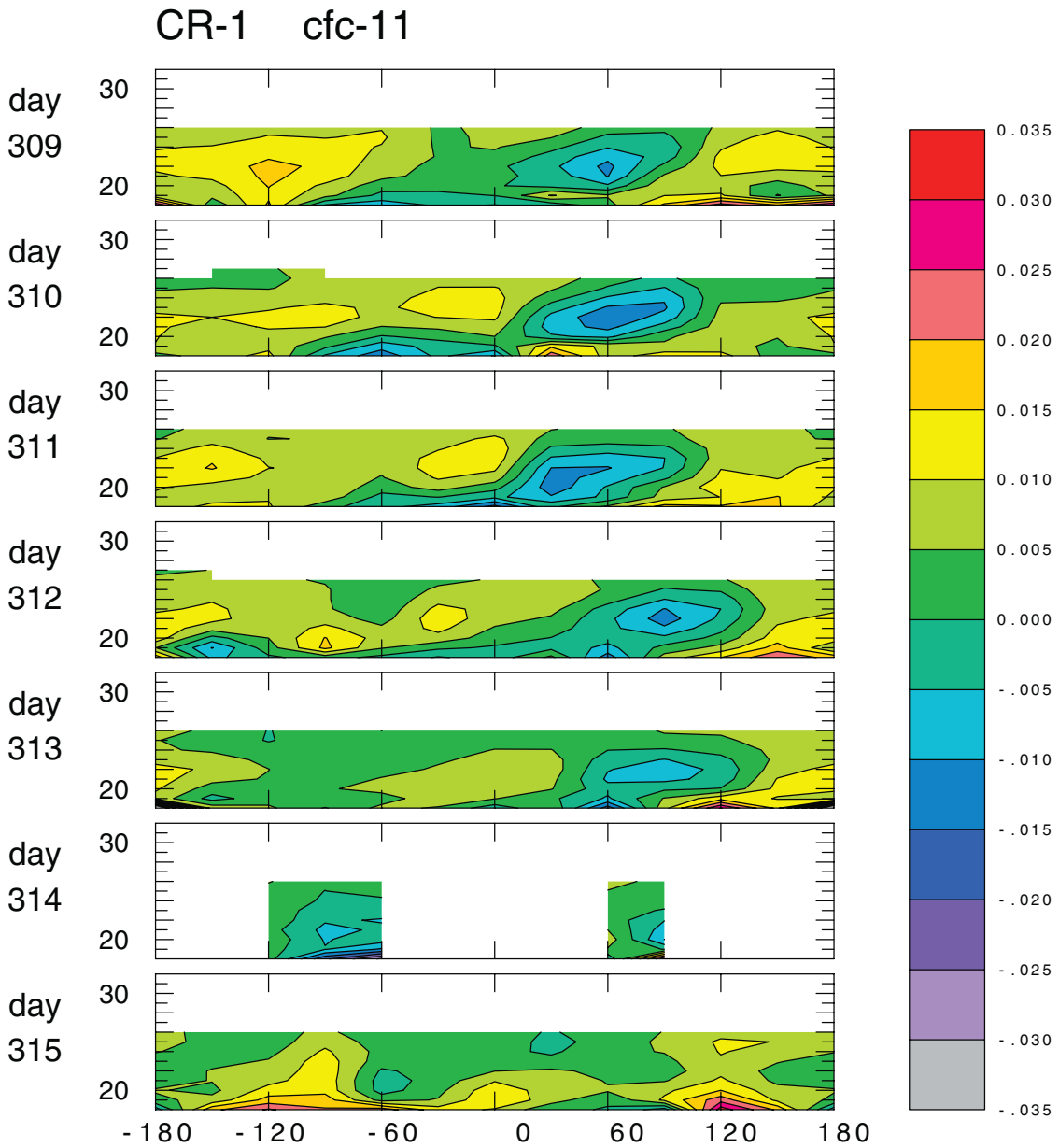

Figure 18. Longitude × altitude cross-sections of CR-1 CFC-11 mixing ratio deviation from the mission mean, averaged over the latitude band 10°S to 10°N. Panels show a sequence of days. Units are ppbv.

[46] Of the constituents currently available in the CRISTA data, we expect to see signatures of vertical transport by Kelvin wave activity in several long-lived tracers: N_2O, CFC-11 (chlorofluorocarbon 11, which is $CFCl_3$), CH_4, HNO_3, and O_3 in the lower stratosphere. In addition, we also expect a signal for ozone in the upper stratosphere due to the strong dependence of ozone photochemistry on temperature. The observed short-lived species, $ClONO_2$ and N_2O_5, are not expected to show simple variation with Kelvin waves and this is confirmed by the observations (not shown). They will not be discussed further.

[47] The relationship of the perturbation field has been shown to take on a simple form under two limiting conditions [*Randel*, 1990]. Where the trace species is approximately conserved and radiative damping can be neglected, the relationship is

$$\frac{\mu'}{T'} = \frac{\bar{\mu}_z}{S} \tag{4}$$

where $S = HN^2/R$, H is the atmospheric scale height, N is the buoyancy frequency, and R is the gas constant for air. Alternatively, for cases when the tracer is approximately in photochemical equilibrium and has a loss rate that varies with temperature, as is the case for ozone above 40 km, the relationship is

$$\frac{\mu'}{T'} = \frac{\bar{\mu}}{\bar{L}} \frac{\partial L}{\partial T} \tag{5}$$

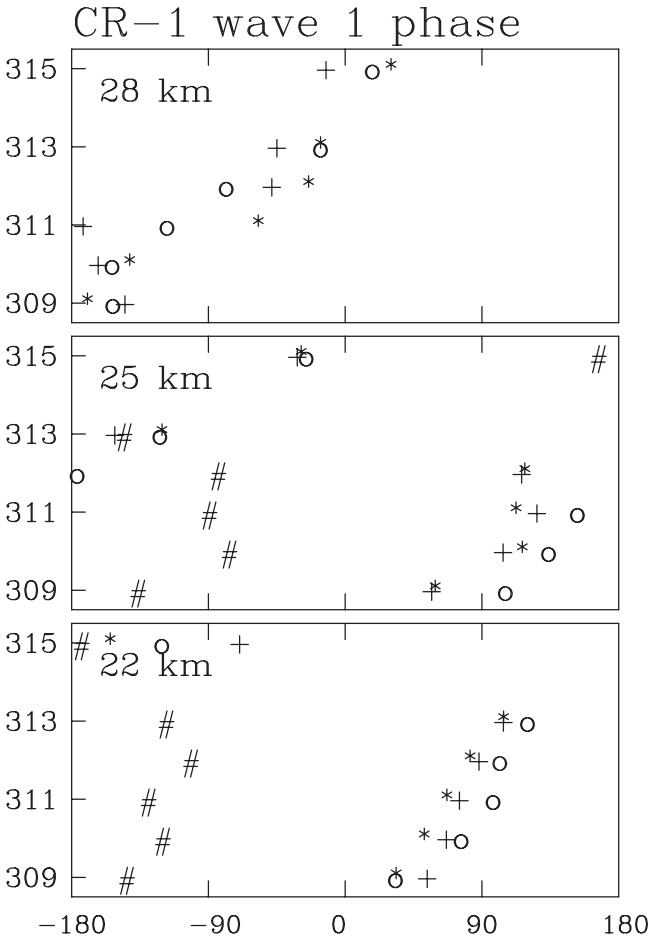

Figure 19. Phase of zonal wave number 1 for temperature (o), ozone (*), nitric acid (+), and CFC-11 (#) at three levels, for each day during CR-1.

where L is the photochemical loss rate. Finally, where the photochemical loss rate becomes important but is not highly dependent on temperature, as is the case for the photochemical destruction of the source gases N_2O, CFC-11, and CH_4 in the region where their lifetimes become less than a week, the ratio μ'/T' takes on an imaginary part, indicating a phase shift between the tracer and temperature perturbations.

$$\frac{\mu'}{T'} = -\frac{(k\bar{u}-\omega)^2 + i(k\bar{u}-\omega)L}{(k\bar{u}-\omega)^2 + L^2}\frac{\bar{\mu}_z}{S} \tag{6}$$

[48] The first limiting case (4) applies approximately in the lower stratosphere for all the trace species considered here. Since S is always positive, this means that μ' will be in phase with T' when the tracer gradient is positive and will be out of phase with T' when the gradient is negative. N_2O, CH_4 and CFC-11 have negative gradients in the middle atmosphere; HNO_3 has a positive gradient to about 28–30 km, and O_3 has a positive gradient to about 30–32 km. N_2O and CH_4 are not shown because the range of the data did not extend into the lower stratosphere where the Kelvin wave was prominent.

[49] Figure 16 shows daily tropical perturbations of ozone during CR-1. The basic structure conforms well to what is predicted by equation (4), i.e., the ozone concentration shows a structure similar to temperature. The structure of HNO_3 variations (Figure 17) is also similar to that of temperature, indicating, as expected, that transport is dominant for both of the species in the lower stratosphere. The lifetimes of O_3 and HNO_3 both become short enough near 30 km that photochemistry should begin to play a role [*Austin et al.*, 1986; *Brasseur and Solomon*, 1986]. However, it is also the case that the gradients of both disappear there, so the impact of Kelvin waves on the concentration is minimal.

[50] Since CFC-11 has a negative vertical gradient over its entire range, we expect perturbations (Figure 18) to be approximately out of phase with those of temperature. However, CFC-11 is rapidly destroyed by photolysis in the stratosphere and its perturbation is then described by equation (6).

[51] The phase relationships are seen more clearly in Figure 19, which shows the wave number 1 phase on each day during CR-1 for temperature, O_3, HNO_3, and CFC-11 at several levels. At all levels, phase of the wave number 1 perturbations in O_3 and HNO_3 are close to those of temperature. CFC-11 perturbations are out of phase at 22 km, where the concentration is high. At 25 km, the CFC-11 concentration is decreasing strongly due to photolytic destruction, and the phase relationship to the temperature perturbation shifts as predicted by equation (6). CFC-11 concentration is not detected at 28 km.

[52] The Kelvin waves in CR-2 were observed in the upper stratosphere and the mesosphere. As noted above, ozone perturbations are predicted to have no correlation with those of temperature in the vicinity of the ozone maximum, around 32 km. Above there, both photochemistry and transport contribute to an anticorrelation of ozone and temperature perturbations. This is seen in the CR-2 ozone (Figure 20). The relationship between temperature and ozone in the CRISTA data has also been investigated by *Ward et al.* [2000].

[53] Concentrations of N_2O and CH_4 are decreasing in the upper stratosphere but still are sufficient to be observed by CRISTA. Their behavior in the presence of a Kelvin wave should be controlled primarily by transport, because the photochemical timescales are long. Figure 21 shows the phases of wave number 1 perturbations in temperature, O_3, N_2O, and CH_4 at several levels during the last six days of CR-2. Ozone perturbations are out of phase with those of temperature, as seen by comparing Figures 7 and 20. The perturbations in N_2O and CH_4 are less regular, but overall tend to be out of phase with the temperature perturbations indicating the variations are dominated by vertical transport.

6. Conclusions

[54] The two flights of the CRISTA instrument have provided some new information about Kelvin waves. Of particular note is the simultaneous presence of several different Kelvin waves at different regions of the atmosphere and different zonal wave numbers. CRISTA also allows a brief but detailed look at the evolution of a Kelvin wave packet as it propagates. Because of its very high

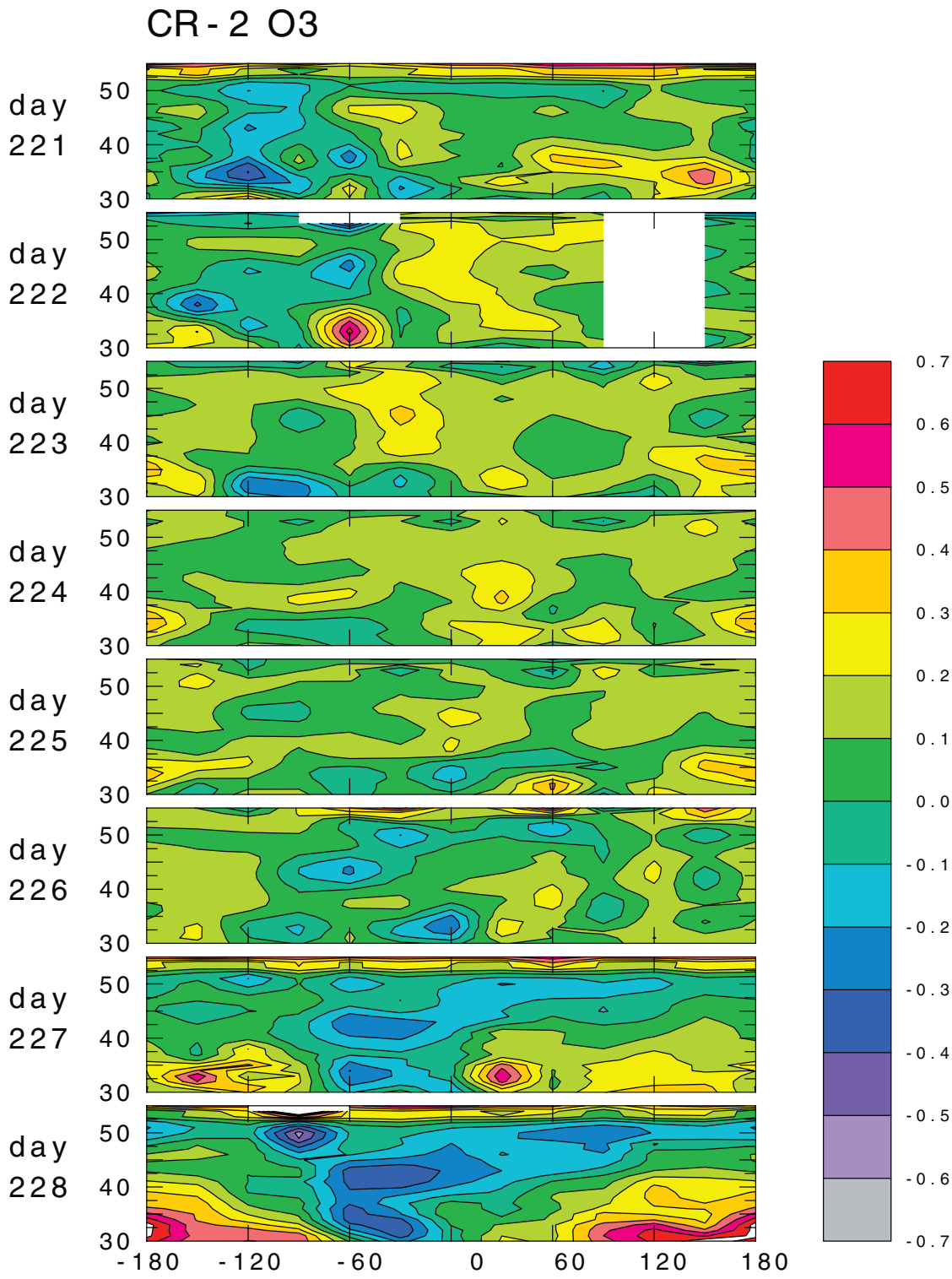

Figure 20. Longitude × altitude cross-sections of CR-2 O_3 mixing ratio deviation from the mission mean, averaged over the latitude band 10°S to 10°N. Panels show a sequence of days. Units are ppmv.

horizontal resolution and its broad vertical range (tropopause to lower thermosphere), the CRISTA data archive allow us to look at wave structures in detail simultaneously over the entire middle atmosphere. The observations show the structure of a wave number 1 Kelvin wave packet (involving more than one frequency) over a very broad range extending from the middle stratosphere to well into the mesosphere. Although the two CRISTA missions lasted for only about 8 days each, multiple Kelvin waves were identified in each mission. A common feature was a tendency for higher-frequency waves to be prominent at higher altitudes. In both missions, a large amplitude Kelvin

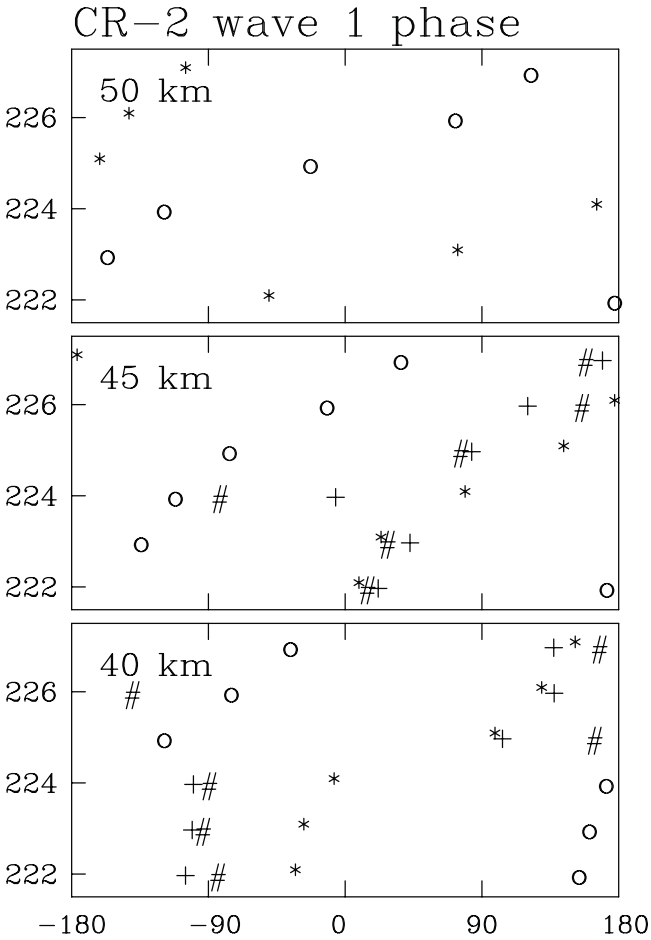

Figure 21. Phase of zonal wave number 1 for temperature (o), ozone (∗), N_2O (+), and CH_4 (#) at two or three levels, for each of the six last days of CR-2.

wave with zonal wave number 1 dominated the perturbation temperature field in the tropics. In CR-1, November 1994, the dominant wave number 1 was seen between 18 and 30 km while in CR-2, August 1997, the wave number 1 Kelvin wave extended from 30 to 70 km.

[55] Using the day to day phase progression and a numerical fitting technique, supported by evidence from the vertical and latitudinal structure, we can identify perturbations as Kelvin waves. During CR-1, wave 1 Kelvin waves were seen with periods of 17 and 11 days, both in the lower stratosphere. Wave 2 was observed to have similar phase speeds, giving periods of 9 and 5 days. There also was an indication of a wave 3 with a similar phase speed to the longer period wave 1 and 2 but, because it did not propagate far into the stratosphere, no supporting evidence for its identification as a Kelvin wave was available. During CR-2, simultaneous Kelvin waves with zonal wave numbers 1 and 2 were again observed. The $k = 1$ wave periods were found to be 13 and 4 days. The observed $k = 2$ wave had a period of about 3.5 days. There is also evidence that an observed wave number 4 perturbation was a Kelvin wave with a 5 day period. Note that the short duration of the CRISTA missions leaves some uncertainties as to the exact frequencies of longer period Kelvin waves.

[56] CRISTA trace species data also show variations in response to the tropical waves. This paper presents the first global observations of the perturbations of trace species in response to a low frequency lower stratospheric Kelvin waves. Ozone, nitric acid, and CFC-11 vary as predicted due to vertical transport. Upper stratospheric trace species (O_3, N_2O and CH_4) also show clear correlations with the temperature perturbations associated with the Kelvin waves. These observations, particularly those of trace species with low concentrations such as CFC-11, are indications of the reliability and unique capabilities of the CRISTA instrument.

[57] **Acknowledgments.** We thank D. Ortland for discussions about this work and extensive comments on the paper. The National Center for Atmospheric Research is operated by the University Corporation for Atmospheric Research under sponsorship of the National Science Foundation. The CRISTA project was supported by the Bundesministerium für Bildung, Forschung und Technologie (BMBFT) through Deutsches Zentrum für Luft- und Raumfahrtangelegenheiten (DLR, formerly DARA). The CRISTA instrument was part of the ATLAS-3 and CRISTA-SPAS missions of the National Aeronautics and Space Administration (NASA).

References

Austin, J., R. R. Garcia, J. M. Russel III, S. Solomon, and A. F. Tuck, On the atmospheric photochemistry of nitric acid, *J. Geophys. Res.*, *91*, 5477–5485, 1986.

Boyd, J. P., Effects of latitudinal shear on equatorial waves, 2, Applications to the atmosphere, *J. Atmos. Sci.*, *35*, 2259–2267, 1978.

Brasseur, G., and S. Solomon, *Aeronomy of the Middle Atmosphere*, 2nd ed., 452 pp., D. Reidel, Norwell, Mass., 1986.

Canziani, P. O., Slow and ultraslow equatorial Kelvin waves, *Q. J. R. Meteorol. Soc.*, *125*, 657–676, 1999.

Canziani, P. O., and J. R. Holton, Kelvin waves and the quasi-biennial oscillation: An observational analysis, *J. Geophys. Res.*, *103*, 31,509–31,521, 1998.

Canziani, P. O., J. R. Holton, E. Fishbein, L. Froidevaux, and J. W. Waters, Equatorial Kelvin waves: A UARS MLS view, *J. Atmos. Sci.*, *51*, 3053–3076, 1994.

Canziani, P. O., J. R. Holton, E. Fishbein, and L. Froidevaux, Equatorial Kelvin wave variability during 1992 and 1993, *J. Geophys. Res.*, *100*, 5193–5202, 1995.

Coy, L., and M. Hitchman, Kelvin wave packets and flow acceleration: A comparison of modeling and observations, *J. Atmos. Sci.*, *41*, 1875–1880, 1984.

Dunkerton, T. J., On the role of the Kelvin wave in the westerly phase of the semiannual oscillation, *J. Atmos. Sci.*, *36*, 32–41, 1979.

Dunkerton, T. J., Theory of the mesopause semiannual oscillation, *J. Atmos. Sci.*, *39*, 2681–2690, 1982.

Ern, M., Relaxationseffekte der CRISTA-Infrarotdetektoren und ihre Korrektur, WUB-DIS 2000-4, Ph.D. thesis, Phys. Dep., Wuppertal Univ. (BUGW), Wuppertal, Germany, 2000.

Garcia, R. R., and M. L. Salby, Transient response to localized episodic heating in the tropics, 2, Far-field behavior, *J. Atmos. Sci.*, *44*, 499–530, 1987.

Garcia, R. R., and F. Sassi, Modulation of the mesospheric semi-annual oscillation by the quasibiennial oscillation, *Earth Planets Space*, *51*, 563–569, 1999.

Garcia, R. R., R. S. Lieberman, T. J. Dunkerton, and R. A. Vincent, Climatology of the semiannual oscillation of the tropical middle atmosphere, *J. Geophys. Res.*, *102*, 26,019–26,032, 1997.

Grossmann, K.-U., et al., The CRISTA 2 Mission: Introduction and overview, *J. Geophys. Res.*, 10.1029/2001JD000667, in press, 2002.

Hirota, I., Kelvin waves in the equatorial middle atmosphere observed with Nimbus 5 SCR, *J. Atmos. Sci.*, *45*, 714–722, 1978.

Hirota, I., Equatorial waves in the upper stratosphere and mesosphere in relation to the semiannual oscillation of the zonal wind, *J. Atmos. Sci.*, *36*, 217–222, 1979.

Hirota, I., M. Shiotani, T. Sakuri, and J. C. Gille, Kelvin waves near the equatorial stratopause as seen in SBUV ozone data, *J. Meteorol. Soc. Jpn.*, *69*, 179–186, 1991.

Hitchman, M. H., and C. B. Leovy, Estimation of the Kelvin wave contribution to the semiannual oscillation, *J. Atmos. Sci.*, *45*, 1462–1475, 1988.

Holton, J. R., and R. S. Lindzen, A note on "Kelvin" waves in the atmosphere, *Mon. Weather Rev.*, *96*, 385–386, 1968.

Holton, J. R., M. J. Alexander, and M. T. Boehm, Evidence for short vertical wavelength Kelvin waves in the DOE-ARM Nauru99 radiosonde data, *J. Geophys. Res.*, *106*, 20,125–20,130, 2001.

Lieberman, R. S., and D. Riggin, High resolution Doppler imager observations of Kelvin waves in the equatorial mesosphere and lower thermosphere, *J. Geophys. Res.*, *102*, 26,117–26,130, 1997.

Oberheide, J., Messung und Modellierung von Gezeitenwellen in der mittleren Erdatmosphaere: Ergebnisse des CRISTA-Experiments, WUB-DIS 2000-10, Ph.D. thesis, Phys. Dep., Wuppertal Univ. (BUGW), Wuppertal, Germany, 2000.

Oberheide, J., G. A. Lehmacher, D. Offermann, K. U. Grossmann, C. E. Meek, A. H. Manson, F. J. Schmidlin, and W. Singer, Geostrophic wind fields in the stratosphere and mesosphere from satellite data, *J. Geophys. Res.*, 10.1029/2001JD000655, in press, 2002.

Offermann, D., K.-U. Grossmann, P. Barthol, P. Knieling, M. Riese, and R. Thant, Cryogenic Infrared Spectrometers and Telescopes for the Atmosphere (CRISTA) experiment and middle atmosphere variability, *J. Geophys. Res.*, *104*, 16,311–16,325, 1999.

Randel, W. J., Kelvin wave-induced trace constituent oscillations in the equatorial stratosphere, *J. Geophys. Res.*, *95*, 18,641–18,652, 1990.

Randel, W. J., and J. C. Gille, Kelvin wave variability in the upper stratosphere observed in SBUV ozone data, *J. Atmos. Sci.*, *48*, 2336–2349, 1991.

Riese, M., P. Preusse, R. Spang, M. Ern, M. Jarisch, K.-U. Grossmann, and D. Offermann, Measurements of trace gases by the Cryogenic Infrared Spectrometers and Telescopes for the Atmosphere (CRISTA) experiment, *Adv. Space Res.*, *19*, 563–566, 1997.

Riese, M., R. Spang, P. Preusse, M. Ern, M. Jarisch, D. Offermann, and K.-U. Grossmann, Cryogenic Infrared Spectrometers and Telescopes for the Atmosphere (CRISTA) data processing and temperature and trace gas retrieval, *J. Geophys. Res.*, *104*, 16,349–16,367, 1999.

Riggin, D. M., D. C. Fritts, T. Tsuda, T. Nakamura, and R. A. Vincent, Radar observations of a 3-day Kelvin wave in the equatorial mesosphere, *J. Geophys. Res.*, *102*, 26,141–26,157, 1997.

Salby, M. L., and R. R. Garcia, Transient response to localized episodic heating in the tropics, 1, Excitation and short-term near-field behavior, *J. Atmos. Sci.*, *44*, 458–498, 1987.

Salby, M. L., D. L. Hartmann, P. L. Bailey, and J. C. Gille, Evidence for equatorial Kelvin modes in Nimbus-7 LIMS, *J. Atmos. Sci.*, *41*, 220–235, 1984.

Salby, M. L., P. Callaghan, S. Solomon, and R. R. Garcia, Chemical fluctuations associated with vertically propagating equatorial Kelvin waves, *J. Geophys. Res.*, *95*, 20,491–20,505, 1990.

Shiotani, M., and T. Horinouchi, Kelvin wave activity and the quasi-biennial oscillation in the equatorial lower stratosphere, *J. Meteorol. Soc. Jpn.*, *71*, 175–182, 1993.

Shiotani, M., J. C. Gille, and A. E. Roche, Kelvin waves in the equatorial lower stratosphere as revealed by cryogenic limb array etalon spectrometer temperature data, *J. Geophys. Res.*, *102*, 26,131–26,140, 1997.

Smith, A. K., and M. Riese, Cryogenic Infrared Spectrometers and Telescopes for the Atmosphere (CRISTA) observations of tracer transport by inertially unstable circulations, *J. Geophys. Res.*, *104*, 19,171–19,182, 1999.

Srikanth, R., and D. A. Ortland, Analysis of Kelvin waves in high-resolution Doppler imager and microwave limb sounder stratosphere measurements using a constrained least squares method, *J. Geophys. Res.*, *103*, 23,131–23,151, 1998.

Takahashi, M., and B. A. Boville, A three-dimensional simulation of the equatorial quasi-biennial oscillation, *J. Atmos. Sci.*, *49*, 1020–1035, 1992.

Takahashi, H., R. A. Buriti, D. Gobbi, and P. P. Batista, Equatorial planetary wave signatures observed in mesospheric airglow emissions, *J. Atmos. Solar Terr. Phys.*, *64*, 1263–1272, 2002.

Wallace, J. M., and V. Kousky, Observational evidence of Kelvin waves in the tropical stratosphere, *J. Atmos. Sci.*, *25*, 900–907, 1968.

Ward, W. E., J. Oberheide, M. Riese, P. Preusse, and D. Offermann, Tidal signatures in temperature data from CRISTA 1 mission, *J. Geophys. Res.*, *104*, 16,391–16,403, 1999.

Ward, W. E., J. Oberheide, M. Riese, P. Preusse, and D. Offermann, Planetary wave two signatures in CRISTA 2 ozone and temperature data, in *Atmospheric Science Across the Stratopause*, edited by D. E. Siskind, S. D. Eckermann, and M. E. Summers, pp. 319–325, AGU, Washington D. C., 2000.

Ziemke, J. R., and J. L. Stanford, Quasi-biennial oscillation and tropical waves in total ozone, *J. Geophys. Res.*, *99*, 23,041–23,056, 1994.

A. K. Smith, Atmospheric Chemistry Division, National Center for Atmospheric Research, P.O. Box 3000, Boulder, CO 80307, USA. (aksmith@ucar.edu)

P. Preusse, Institute for Chemistry and Dynamics of the Geosphere (ICG), Institute I: Stratosphere, Forchungszentrum Jülich, D-52425 Jülich, Germany. (p.preusse@fz-juelich.de)

J. Oberheide, High Altitude Observatory, National Center for Atmospheric Research, P.O. Box 3000, Boulder, CO 80307, USA. (jenso@ucar.edu)